



**LOCAL AERODYNAMIC PARAMETERS FOR SUPERSONIC  
AND HYPERSONIC FLUTTER ANALYSES**

*JAMES J. OLSEN*

**Distribution of this Document is Unlimited**

## FOREWORD

This report covers research conducted from 1 July 1964 to 1 April 1965 by the Air Force Flight Dynamics Laboratory, Vehicle Dynamics Division, Aerospace Dynamics Branch.

The work was performed to advance the state-of-the-art of flutter prediction for flight vehicles as part of the Research and Technology Division, Air Force Systems Command's exploratory development program. This research was conducted under Project No. 1370 "Dynamic Problems in Flight Vehicles," and Task No. 137003, "Prediction and Prevention of Aerothermoelastic Instabilities." Mr. James J. Olsen of the Vehicle Dynamics Division, Air Force Flight Dynamics Laboratory, was the Project Engineer.

The manuscript for this report was released by the author in April 1965.

This report has been reviewed and is approved.

*Walter J. Markytow*  
WALTER J. MARKYTOW

Asst. for Research & Technology  
Vehicle Dynamics Division

## ABSTRACT

This report presents the results of an analysis to determine how certain aerodynamic flutter parameters ( $M$ ,  $q$ ,  $q/\beta$ ) are changed from their free stream values by the existence of supersonic and hypersonic nose shock waves and expansions. The results indicate that nose shock waves and expansions can create a new set of "free stream" conditions for flutter analyses. These new free stream conditions can be sufficiently different from the undisturbed "free stream" condition to warrant their detailed analyses in the supersonic and hypersonic vehicle.

## CONTENTS

Section		Page
	Introduction	1
I	The Sharp Wedge	3
II	Bluntness Effects	7
III	Intermediate Regions	11
IV	Conclusions	16
	References	18

## LIST OF ILLUSTRATIONS

Figure		Page
1(a)	Local Mach Number vs Compression Angle, Oblique Shock Theory . . . . .	19
1(b)	Local Mach Number vs Compression Angle, Oblique Shock Theory . . . . .	20
1(c)	Local Mach Number vs Compression Angle, Oblique Shock Theory . . . . .	21
2(a)	Ratio of Local Dynamic Pressure to Free Stream Dynamic Pressure vs Compression Angle, Oblique Shock Theory . . . . .	22
2(b)	Ratio of Local Dynamic Pressure to Free Stream Dynamic Pressure vs Compression Angle, Oblique Shock Theory . . . . .	23
3(a)	Ratio of $(q/\beta)_L$ to $(q/\beta)_\infty$ vs Compression Angle, Oblique Shock Theory . . . . .	24
3(b)	Ratio of $(q/\beta)_L$ to $(q/\beta)_\infty$ vs Compression Angle, Oblique Shock Theory . . . . .	25
4(a)	Local Mach Number vs Expansion Angle, Prandtl-Meyer Expansion . . . . .	26
4(b)	Local Mach Number vs Expansion Angle, Prandtl-Meyer Expansion . . . . .	27
5(a)	Ratio of Local Dynamic Pressure to Free Stream Dynamic Pressure vs Expansion Angle, Prandtl-Meyer Expansion . . . . .	28
5(b)	Ratio of Local Dynamic Pressure to Free Stream Dynamic Pressure vs Expansion Angle, Prandtl-Meyer Expansion . . . . .	29
6(a)	Ratio of $(q/\beta)_L$ to $(q/\beta)_\infty$ vs Expansion Angle, Prandtl-Meyer Expansion . . . . .	30
6(b)	Ratio of $(q/\beta)_L$ to $(q/\beta)_\infty$ vs Expansion Angle, Prandtl - Meyer Expansion . . . . .	31

LIST OF ILLUSTRATIONS  
(Cont'd)

Figure		Page
7	Correlation of Simple and Modified Forms of Newtonian Theory with Experimental Results . . . . .	32
8	Local Mach Number vs Local Angle of Attack, Modified Newtonian Theory . . . . .	33
9(a)	Ratio of Local Dynamic Pressure to Free Stream Dynamic Pressure vs Local Angle of Attack, Modified Newtonian Theory . . . . .	34
9(b)	Ratio of Local Dynamic Pressure to Free Stream Dynamic Pressure vs Local Angle of Attack, Modified Newtonian Theory . . . . .	35
10	Ratio of $(q/\beta)_I$ to $(q/\beta)_\infty$ vs Local Angle of Attack, Modified Newtonian Theory . . . . .	36
11	The Dependence of Local Pressure on the Location of the Newtonian-Blast Theory Matching Point . . . . .	37
12	Local Mach Number vs the Matching Parameter, Blast Wave Theory Matched with Newtonian Theory . . . . .	38
13	The Ratio of Local Dynamic Pressure to Free Stream Dynamic Pressure vs the Matching Parameter $\epsilon$ , Blast Wave Theory Matched with Newtonian Theory . . . . .	39
14	The ratio $(q/\beta)_I$ to $(q/\beta)_\infty$ vs the Matching parameter $\epsilon$ , Blast Wave Theory Matched with Newtonian Theory. . . . .	40

## SYMBOLS

Symbol	
$C_{DN}$	Nose drag coefficient
$C_P$	Pressure coefficient, $\frac{P - P_\infty}{q_\infty}$
D	Nose diameter
E	Modulus of elasticity
$f_o(\gamma)$	Function of $\gamma$
F	Dimensionless flutter parameter
h	Thickness
L	Length
M	Mach number
P	Pressure
q	Dynamic pressure, $1/2 \rho V^2$
S	Distance downstream from nose
V	Velocity
W	Width
x	Cartesian coordinate
$\beta$	$\sqrt{M^2 - 1}$
$\gamma$	Ratio of specific heats, 1.4
$\delta$	Angle of Compression or expansion
$\epsilon$	Abbreviation used in Blast Wave Theory
$\rho$	Density
$\theta$	Shock wave angle

SYMBOLS (Cont'd)

Subscripts

$\infty$	Free stream
L	Local
m	Matched point
T	Stagnation condition
1	Behind oblique shock

## INTRODUCTION

The advent of sustained supersonic flight was accompanied by a whole host of new problems, among them aerodynamic heating and increased drag. Another new problem, not so well publicized but still important, was panel flutter.

Under certain conditions of Mach number and dynamic pressure, it is possible for skin panels of aircraft and missiles to experience self-sustained vibrations. The vibrations are known as panel flutter and can cause immediate catastrophic failure or long term fatigue damage, depending upon edge conditions, structural nonlinearities and the severity of the flight environment. The most severe aerodynamic environment is generally considered to be one of high dynamic pressure and/or Mach number near 1.0.

Our ability to predict the exact conditions under which panel flutter will occur is currently rather poor because of many aerodynamic and structural uncertainties. The structural uncertainties stem from the thinness and inherent nonlinearity of the skin panels of interest. The thin panels usually are extremely sensitive to small changes in temperature, edge conditions, differential pressurization, and midplane stresses. As a result, the structural properties are not always well defined and are disturbed by small changes in the important parameters. The aerodynamic uncertainties arise from a lack of satisfactory methods to predict oscillatory pressures on vibrating surfaces, particularly in transonic and low supersonic viscous flow.

As satisfactory theoretical methods evolve and as data become available from well controlled experiments, our ability to predict panel flutter should improve. However, it will then be necessary to devise means of interpreting data from analyses and experiments in terms of the actual conditions on aircraft and missiles in flight, i.e., the "local" conditions.

The purpose of this report is to take a first step in that direction and to show how "local" conditions can be at large variance from the nominal "free stream" conditions. With this type of information, the aircraft designer will be able to use the free stream parameters such as Mach number, dynamic pressure and angle of attack to predict the "local" Mach number and "local" dynamic pressure at the regions of interest. These "local" conditions should then be the proper parameters to use as a measure of the severity of the flight environment for flutter.

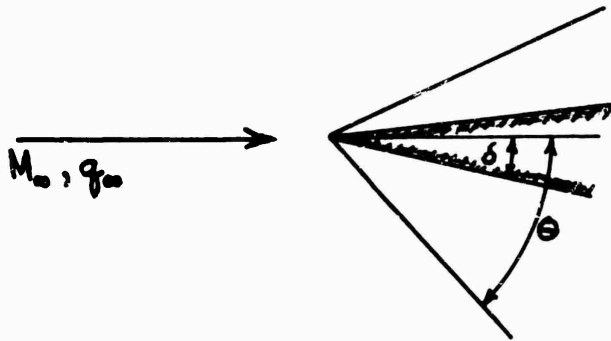
Section I develops the "local" conditions on a two dimensional sharp wedge in a supersonic flow of a perfect gas. Section II shows how the effects of nose bluntness can drastically change these "local"

conditions. Section III combines Newtonian flow theory and Sakurai's blast theory to obtain "local" conditions on aft positions of blunt surfaces. Section IV summarizes the conclusions obtained.

## SECTION I

### THE SHARP WEDGE

The object of this section is to determine how the local aerodynamic conditions, particularly Mach number and dynamic pressure, are changed as the free stream flow is altered by the presence of a sharp, two dimensional wedge. (See sketch below) Consider the flow of a perfect gas, defined by the free stream conditions  $M_\infty$  and  $q_\infty$ . The flow is deflected through an angle  $\delta$ , causing the attached,



straight shock wave at an angle  $\theta$ . As a result of the shock wave, the Mach number and dynamic pressure are changed from  $M_\infty$  and  $q_\infty$  to the "local" conditions  $M_L$  and  $q_L$ . The most convenient method of calculation is an inverse one in that we assume values for  $M_\infty$  and  $\theta$ , then calculate the corresponding values for  $\delta$ . Using the equations from NACA TR 1135, reference (1), we have for  $\gamma = 1.4$ :

$$\cot \delta = \tan \theta \left( \frac{1.2M_\infty^2}{M_\infty^2 \sin^2 \theta - 1} - 1 \right) \quad (1.1)$$

Also, for the local Mach number and the ratio of the local pressure to free stream pressure, we have:

$$M_L = \left[ \frac{36M_\infty^4 \sin^2 \theta - 5 (M_\infty^2 \sin^2 \theta - 1)(7M_\infty^2 \sin^2 \theta + 5)}{(7M_\infty^2 \sin^2 \theta - 1)(M_\infty^2 \sin^2 \theta + 5)} \right]^{1/2} \quad (1.2)$$

$$\frac{P_L}{P_\infty} = \frac{7M_\infty^2 \sin^2 \theta - 1}{6} \quad (1.3)$$

For a perfect gas, the ratio of local dynamic pressure to free stream dynamic pressure is:

$$\frac{q_L}{q_\infty} = \frac{\rho_L V_L^2}{\rho_\infty V_\infty^2} = \frac{P_L M_L^2}{P_\infty M_\infty^2} \quad (1.4)$$

Inserting equations (1.2) and (1.3) into (1.4) we get:

$$\frac{q_L}{q_\infty} = \frac{36M_\infty^4 \sin^2\theta - 5(M_\infty^2 \sin^2\theta - 1)(7M_\infty^2 \sin^2\theta + 5)}{6M_\infty^2 (M_\infty^2 \sin^2\theta + 5)} \quad (1.5)$$

The results obtained are illustrated in Figures (1) to (3).

Figures (1a) to (1c) show the effect of a two dimensional oblique shock on the local Mach number. The value of  $M_L$  starts at the value of  $M_\infty$  for  $\delta$  equal to zero. As  $\delta$  is increased,  $M_L$  then proceeds to decrease to the point where further increases in  $\delta$  would cause shock detachment. Thus  $M_L$  is less than or equal to  $M_\infty$  for all  $\delta$ . Since flutter problems tend to be most critical for  $M = 1$ , one would then conclude that increases in  $\delta$  would tend to increase the potential for flutter instabilities.

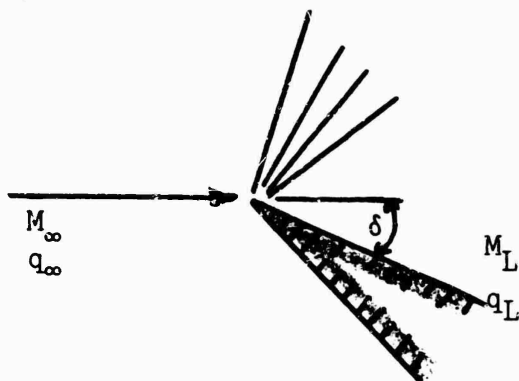
Figures (2a) and (2b) show the effect of a two dimensional oblique shock on the local dynamic pressure. The ratio  $q_L/q_\infty$  is plotted against  $\delta$  for several values of  $M_\infty$ . As  $\delta$  is increased from zero, the ratio  $q_L/q_\infty$  increases at first but then decreases to a value approximately equal to 1.0 as shock detachment is approached. Since flutter problems tend to be most severe at high levels of  $q$ , one could then conclude that increases in  $\delta$  would increase the potential for flutter instabilities only at first and that further increases in  $\delta$  would tend to be stabilizing. Note for  $M_\infty$  less than 1.5 that  $q_L/q_\infty$  is always less than or equal to 1.0.

It is apparent that the effects of  $\delta$  on flutter stability should not be judged from the effects on  $M$  or  $q$  alone. In an attempt to combine the possibly conflicting effects figures (3a) and (3b) were prepared. Figures (3a) and (3b) illustrate the effect of  $\delta$  on the ratio  $\frac{(q/\beta)_L}{(q/\beta)_\infty}$  from several values of  $M_\infty$ . As can be seen,

$\frac{(q/\beta)_L}{(q/\beta)_\infty}$  increases in  $\delta$  from  $0^\circ$  up to shock detachment cause the local value of  $(q/\beta)$  to increase substantially over the corresponding free stream value: The parameter  $q/\beta$  loses its validity as  $M \rightarrow 1$ , so the extremely high values of the ratio  $(q/\beta)_L / (q/\beta)_\infty$  as  $M_L \rightarrow 1$  in figures 3, 10, and 14 should not be given too much physical significance.

Now, it can be shown that the stiffness required in a skin panel to prevent flutter is roughly proportional in some manner to  $q/\beta$ . Thus, one can conclude that oblique shock theory always predicts that increases in  $\delta$  are destabilizing since increases in  $\delta$  always increase  $q/\beta$ .

In addition to shock wave effects, the possibility of supersonic expansion should also be considered. If the wedge is at a large angle of attack the upper surface will be in an expansion zone and can be analyzed by means of the classical Prandtl-Meyer expansion equations (see sketch below).



The flow is turned through an angle  $\delta$ , resulting in local conditions  $M_L$  and  $q_L$ . As with the oblique shock case, the most convenient method of calculation is an inverse one. Values are initially assumed for  $M_L$  and  $M_\infty$  and the corresponding  $\delta$  is obtained from the equations of reference (1).

$$\delta = \sqrt{6} \left( \tan^{-1} \sqrt{\frac{M_L^2 - 1}{6}} - \tan^{-1} \sqrt{\frac{M_\infty^2 - 1}{6}} \right) - \left( \tan^{-1} \sqrt{M_L^2 - 1} - \tan^{-1} \sqrt{M_\infty^2 - 1} \right) \quad (1.6)$$

Now to evaluate the local static pressure,  $p_L$ , we use the usual equations for the relationship between static pressure and stagnation pressure:

$$\frac{P_{T_L}}{P_L} = \left( 1 + \frac{M_L^2}{5} \right)^{7/2} \quad (1.7)$$

$$\frac{P_{T_\infty}}{P_\infty} = \left( 1 + \frac{M_\infty^2}{5} \right)^{7/2} \quad (1.8)$$

Since the expansion is an isentropic process:

$$P_{T_L} = P_{T_\infty} \quad (1.9)$$

$$\frac{P_L}{P_\infty} = \left[ \frac{5 + M_\infty^2}{5 + M_L^2} \right]^{7/2} \quad (1.10)$$

Equation (1.4) then gives:

$$\frac{q_L}{q_\infty} = \frac{M_L^2}{M_\infty^2} \left[ \frac{5 + M_\infty^2}{5 + M_L^2} \right]^{7/2} \quad (1.11)$$

The results obtained from the Prandtl-Meyer expansion are illustrated in figures (4) to (6).

Figures (4a) and (4b) illustrate how the local Mach number changes as the expansion angle is increased for several values of the free stream Mach number. As would be expected from previous well known results, the effect of increasing  $\delta$  is to cause  $M_L$  to be greater than or equal to  $M_\infty$  in all instances. This effect should then be a stabilizing one, insofar as the flutter of a skin panel is concerned.

Figures (5a) and (5b) are plots of the ratio  $q_L/q_\infty$  vs  $\delta$  for several values of  $M_\infty$ . Except for  $M_\infty$  less than 1.3,  $q_L$  is less than  $q_\infty$  for all values of  $\delta$ . Thus, this effect of  $\delta$  is generally a stabilizing one.

As with the oblique shock results, we now specify that the ratio  $(q/\beta)$  is a legitimate one to assess the true severity of the flutter problem. Figures (6a) and (6b) show the ratio

$$\frac{(q/\beta)_L}{(q/\beta)_\infty}$$

vs  $\delta$  for several values of  $M_\infty$ .

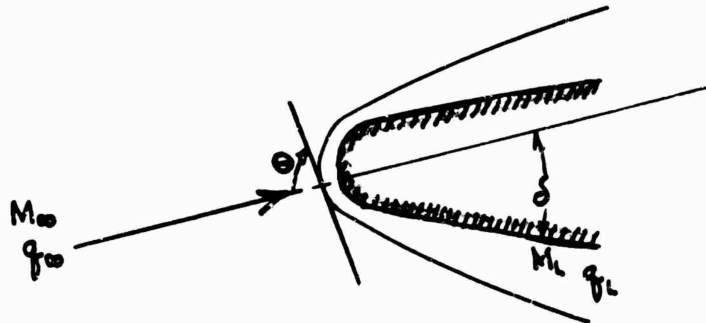
As can readily be seen, the combined effect of  $\delta$  on  $M_L$  and  $q_L$  is to be a stabilizing influence; that is,  $(q/\beta)_L$  is always less than or equal to  $(q/\beta)_\infty$ .

## SECTION II

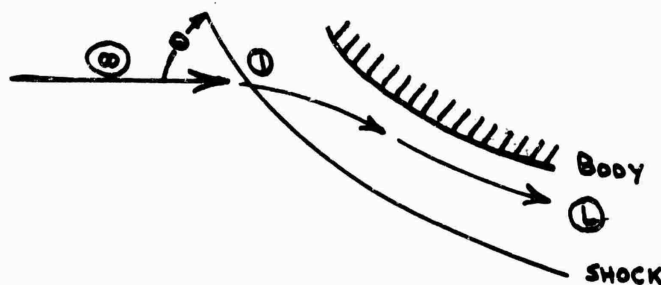
### BLUNTNESS EFFECTS

The purpose of this section is to show how the results of the previous section (sharp wedge) can be drastically altered when the nose is considered to be blunt rather than sharp.

In the sketch below we have a blunted surface which is subject to some supersonic free stream Mach number



and free stream dynamic pressure. We want to find  $M_L$  and  $q_L$  somewhere on the surface. Consider a streamline passing through the strong, curved shock in the sketch below. Let conditions just ahead of the shock be denoted by the subscript  $\infty$  and the conditions just behind



the shock be denoted by the numeral 1. Let the conditions at some point further aft be denoted by the subscript L.

Using two dimensional oblique shock theory for a perfect gas with  $\gamma = 1.4$ , we have:

$$\frac{P_{T1}}{P_\infty} = \left[ \frac{6}{7M_\infty^2 - 1} \right]^{5/2} \left[ \frac{6M_\infty^2 \sin^2 \theta (M_\infty^2 + 5)}{5(M_\infty^2 \sin^2 \theta + 5)} \right]^{7/2} \quad (2.1)$$

Now if we assume that the thermodynamic process from point 1 to point L is isentropic, then

$$P_{T_1} = P_{T_L} \quad (2.2)$$

$P_{T_L}$  is related to  $P_L$  by the isentropic equation

$$\frac{P_L}{P_{T_L}} = \left[ \frac{5}{5 + M_L^2} \right]^{7/2} \quad (2.3)$$

or

$$M_L^2 = 5 \left[ \frac{P_{T_L}}{P_L} \right]^{2/7} - 5 \quad (2.4)$$

Thus the local Mach number,  $M_L$ , is specified by the ratio  $P_{T_L}/P_L$ .

It would be convenient to have  $M_L$  in terms of  $P_L/P_\infty$ . We can do this by further manipulation.

$$\frac{P_{T_L}}{P_L} = \frac{P_{T_1}}{P_L} = \left[ \frac{P_{T_1}}{P_\infty} \right] \cdot \left[ \frac{P_\infty}{P_L} \right] \quad (2.5)$$

The ratio  $\frac{P_{T_1}}{P_\infty}$  is given by equation (2.1). Combining equations

(2.4), (2.5), and (2.1) results in:

$$M_L^2 = \left[ \frac{21.575 M_\infty^2 (M_\infty^2 + 5) \sin^2 \theta}{(M_\infty^2 \sin^2 \theta + 5)(7M_\infty^2 \sin^2 \theta - 1)^{5/7} (P_L/P_\infty)^{2/7}} \right] - 5 \quad (2.6)$$

From the definition of dynamic pressure we have:

$$\frac{q_L}{q_\infty} = \frac{P_L}{P_\infty} \left[ \frac{M_L}{M_\infty} \right]^2 \quad (2.7)$$

Thus, if we know  $M_\infty$ ,  $\theta$ , and the static pressure ratio  $P_L/P_\infty$  we can find  $M_L$  and  $q_L$  from equations (2.6) and (2.7). The only restriction we have made is that the streamline pass through a two dimensional shock and proceed isentropically from there.

At this point it is helpful to observe that the streamline that defines the shape of a blunt body passes through a nearly normal shock. By setting  $\theta \approx 90^\circ$  in equation (2.6) we have:

$$M_L^2 \approx \left[ \frac{21.575 M_\infty^2}{(7M_\infty^2 - 1)^{5/7} (P_L/P_\infty)^{2/7}} \right]^{-5} \quad (2.8)$$

At this point, the ratio  $P_L/P_\infty$  is still not specified. Reference (2) gives a modified form of Newtonian flow theory which uses an empirical correction to fit experimental data over a wide range of  $\delta$ . The form used is:

$$C_p = \left[ 0.82 + \frac{1}{\sqrt{\sin(\delta + 1^\circ)}} \right] \sin^2 \delta \quad (2.9)$$

This compares with the simplest form of Newtonian theory.

$$C_p = 2 \sin^2 \delta \quad (2.10)$$

A comparison of equations (2.9) and (2.10) is shown in figure (7) along with pressure data taken from reference (2). The empirically modified form of Newtonian theory fits the experimental data well over a wide range of  $\delta$ . The remainder of this section will use equation (2.9) to predict the local pressure from:

$$C_p = \frac{P_L - P_\infty}{q_\infty} = \frac{P_L - P_\infty}{.7 P_\infty M_\infty^2} \quad (2.11)$$

$$\frac{P_L}{P_\infty} = .7 C_p M_\infty^2 + 1 \quad (2.12)$$

Combining equations (2.9) and (2.12) results in:

$$\frac{P_L}{P_\infty} = 1 + 0.7 M_\infty^2 \sin^2 \delta \left[ 0.82 + \frac{1}{\sqrt{\sin(\delta + 1^\circ)}} \right] \quad (2.13)$$

Equation (2.8) becomes:

$$M_L^2 = \frac{21.575 M_\infty^2}{(7M_\infty^2 - 1)^{5/7} \left\{ 1 + .7M_\infty^2 \sin^2 \delta \left( .82 + \frac{1}{\sqrt{\sin(\delta + 1^\circ)}} \right) \right\}^{2/7}}^{-5} \quad (2.14)$$

The results of equations (2.7) through (2.14) are shown in figures (8) through (10). We repeat that the basic requirements are that the flow is two dimensional, the governing shock wave is a nearly normal one, the flow is isentropic behind the shock, and the local pressure is given by the empirically modified form of Newtonian theory.

Figure (8) is a plot of the local Mach number vs local angle of attack for several values of free stream Mach number. Note the extremely rapid decrease in  $M_L$  as  $\delta$  is increased above zero. This figure should be compared with figure (1) which was for oblique shock theory. The strong effects of the detached shock cause the Mach number behind the blunt nose to be lower than the corresponding value behind the sharp nose. From figure (8), one would conclude that the local Mach number behind a blunt nose is much more likely to be near transonic than the Mach number behind a sharp nose at the same nominal free-stream conditions. Based on this result, panel flutter tendencies might be thought to be more pronounced.

Figures (9a) and (9b) are plots of  $q_L/q_\infty$  vs  $\delta$  for several values of  $M_\infty$ . As can be seen, the strong shock decreases the local dynamic pressure to such an extent that it never attains its original free-stream value. The loss in velocity through the shock is never compensated for by the corresponding increase in density. This effect would tend to be an alleviating one for flutter and conflicts with the destabilizing effect on Mach number. It is therefore again necessary to look at the behavior of the parameter  $q/\beta$ .

Figure (10) is a plot of  $\frac{(q/\beta)_L}{(q/\beta)_\infty}$  vs  $\delta$  for several values of  $M_\infty$ .

It appears that  $(q/\beta)_L$  is always greater than  $(q/\beta)_\infty$  for all values of  $\delta$  greater than  $10^\circ$  or so. Thus the effect of the strong shock in decreasing the Mach number toward transonic more than offsets its effect in alleviating the dynamic pressure. Figure (10) should be compared with figure (3) which was for oblique shock theory. In general, the  $(q/\beta)$  for a blunt nose is substantially less than the  $(q/\beta)$  predicted by oblique shock theory.

### SECTION III

#### INTERMEDIATE REGIONS

The purpose of the section is to obtain predictions of local Mach number and dynamic pressure in regions between the nose and aft end of a surface where the results of Sections I and II do not apply.

The results of Section I apply only to the faces of a sharp two dimensional wedge. They also have some application to the aft regions of blunt surfaces since the oblique shock results can tend to act as an "upper" boundary condition on those flows. (See sketch)



Oblique Shock Regions

The results of Section II apply only where the modified form of Newtonian theory is valid, i. e., in the vicinity of considerable bluntness. (See sketch)



Newtonian Region

It is possible, within a certain approximation, to use blast theory to get some indication of the local conditions in the intermediate region between the nose and the aft end of a blunt surface. For instance, one of many forms of blast theory is the following (See references 3 and 4)

$$\frac{P_L}{P_\infty} \approx 1 + \frac{f_0(\gamma) M_\infty^2 C_{DN}^{2/3}}{(S_L/D)^{2/3}} \quad (3.1)$$

Where:  $f_0(\gamma) =$  function of  $\gamma$

$C_{D_N}$  = nose drag coefficient

$S_L$  = distance from nose

$D$  = nose diameter

If we want to compare  $P_L$  with  $P_m$  at some other point  $m$  on the same surface we have:

$$\frac{P_L - P_\infty}{P_m - P_\infty} \sim \left[ \frac{S_m}{S_L} \right]^{2/3} \quad (3.2)$$

or

$$\frac{P_L}{P_\infty} = \left[ \frac{S_m}{S_L} \right]^{2/3} \left[ \frac{P_m}{P_\infty} - 1 \right] + 1 \quad (3.3)$$

Thus, if we know the pressure ratio,  $P_m/P_\infty$  at some reference point  $m$ , we can find the local pressure ratio at the other point in question by applying equation (3.3). If we choose the point  $m$  on the nose, we then can apply the modified form of Newtonian theory at  $m$ , match the blast wave solution at that point, and use equation (3.3) to get  $P_L/P_\infty$ .

Let the local angle of attack at the nose "matching point" be  $\delta_m$ . Then, from modified Newtonian theory:

$$\frac{P_m}{P_\infty} - 1 = .7M_\infty^2 \sin^2 \delta_m \left[ 0.82 + \frac{1}{\sqrt{\sin(\delta_m + 1^\circ)}} \right] \quad (3.4)$$

then

$$\frac{P_L}{P_\infty} = 1 + \left( \frac{S_m}{S_L} \right)^{2/3} \left\{ .7M_\infty^2 \sin^2 \delta_m \left[ 0.82 + \frac{1}{\sqrt{\sin(\delta_m + 1^\circ)}} \right] \right\} \quad (3.5)$$

Now maintaining our earlier assumption that the flow is isentropic behind the initial shock wave we have

$$M_L^2 = 5 \left[ \left( \frac{P_{T_L}}{P_L} \right)^{2/7} - 1 \right] \quad (3.6)$$

and  $P_{T_L} = P_{T_1} = \text{constant}$  everywhere behind the initial nose shock wave.

Then

$$M_L^2 = 5 \left[ \left( \frac{P_{T_1}}{P_L} \right)^{2/7} - 1 \right] = 5 \left[ \left( \frac{P_{T_1}}{P_\infty} \right)^{2/7} \left( \frac{P_\infty}{P_L} \right)^{2/7} - 1 \right] \quad (3.7)$$

Again,  $P_{T_1}/P_\infty$  is given by equation (2.1),

$$\frac{P_{T_1}}{P_\infty} = \left[ \frac{6}{7M_\infty^2 - 1} \right]^{5/2} \left[ \frac{6M_\infty^2 \sin^2 \theta (M_\infty^2 + 5)}{5(M_\infty^2 \sin^2 \theta + 5)} \right]^{7/2} \quad (3.8)$$

Noting again the fact that the nose shock wave angle at the streamline that defines the body shape is nearly  $90^\circ$ :

$$\frac{P_{T_1}}{P_\infty} = \left[ \frac{6}{7M_\infty^2 - 1} \right]^{5/2} \left[ \frac{6M_\infty^2}{5} \right]^{7/2} \quad (3.9)$$

Combining equations (3.9) and (3.7) results in:

$$M_L^2 = \frac{21.575 M_\infty^2}{\left( \frac{P_L}{P_\infty} \right)^{2/7} (7M_\infty^2 - 1)^{5/7}} - 5 \quad (3.10)$$

The equation for the ratio  $q_L/q_\infty$  is:

$$\frac{q_L}{q_\infty} = \frac{P_L}{P_\infty} \left( \frac{M_L}{M_\infty} \right)^2 \quad (3.11)$$

Inserting equation (3.10) into (3.11) results in

$$\frac{q_L}{q_\infty} = 5 \left( \frac{P_L}{P_\infty} \right) \left[ \frac{6}{5} \left( \frac{6}{7M_\infty^2 - 1} \right)^{5/7} \left( \frac{P_\infty}{P_L} \right)^{2/7} - 1 \right] \quad (3.12)$$

Here we repeat equation (3.5) for future reference:

$$\frac{P_L}{P_\infty} = \left( \frac{S_m}{S_L} \right)^{2/3} \left\{ .7M_\infty^2 \sin^2 \delta_m \left[ 0.82 + \frac{1}{\sqrt{\sin(\delta_m + 1^\circ)}} \right] \right\} + 1 \quad (3.5)$$

Thus, if we know the distance ratio  $S_m/S_L$ , the local angle of attack at the "match point", and the free-stream Mach number, we can calculate  $P_L/P_\infty$  from equation (3.5). With that result we can use equation (3.10) to get  $M_L$  and equation (3.12) to get  $q_L/q_\infty$ .

For the purpose of simplifying the equations in this section we use the following abbreviation. We let

$$\epsilon = \left( \frac{S_m}{S_L} \right)^{2/3} \left\{ .7 \sin^2 \delta_m \left[ 0.82 + \frac{1}{\sqrt{\sin(\delta_m + 1^\circ)}} \right] \right\} \quad (3.13)$$

Equation (3.5) then becomes:

$$\frac{P_L}{P_\infty} = 1 + M_\infty^2 \epsilon \quad (3.14)$$

Equation (3.10) becomes:

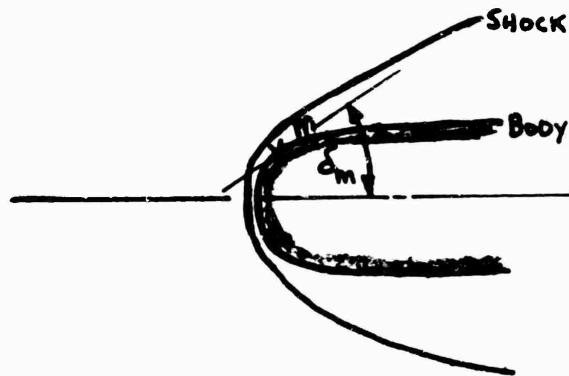
$$M_L^2 = \frac{21.575 M_\infty^2}{(1 + M_\infty^2 \epsilon)^{2/7} (7M_\infty^2 - 1)^{5/7}} - 5 \quad (3.15)$$

Thus, the values of  $P_L/P_\infty$ ,  $M_L$ , and  $q_L/q_\infty$  are functions only of  $M_\infty$  and the parameter  $\epsilon$ . Note that  $\epsilon$  is a function of  $\delta_m$  (the slope at the nose "matching point") and the ratio  $S_L/S_m$  (the ratio of the downstream distance of point L to that of m). If one assumes that he starts at some initial value of  $S_L/S_m$  and then proceeds downstream,  $\epsilon$  is seen to decrease from some initial value toward zero.

It is easy to see from equation (3.14) that  $\epsilon$  is simply related to the local pressure coefficient:

$$\epsilon = \frac{\left( \frac{P_L}{P_\infty} - 1 \right)}{M_\infty^2} = .7C_{P_L} \quad (3.16)$$

Thus, if we refer to equation (3.13) and assume several locations for the matching point m we get several corresponding values for  $\epsilon$ . (See sketch)



The results of this calculation are shown in figure (11). From equation (3.13) we find that

$$\epsilon (S_L/S_m)^{2/3} = .7C_{P_L} (S_L/S_m)^{2/3}$$

is a simple function of the location of the matching point and that the local pressure is completely dominated by the location of the matching point. Thus, given some location of the matching point we can specify the quantity

$C_{P_L} (S_L/S_m)^{2/3}$  and then calculate  $C_{P_L}$  for given values of  $(S_L/S_m)$ . The results of these calculations are shown in figures (12) to (14). Because of the important role of the location of the matching point,  $\epsilon$  is left unspecified, and the curves are plotted vs  $\epsilon$ .

Figure (12) is a plot of local Mach number vs  $\epsilon$  for several values of the free stream Mach number. Remember that  $\epsilon$  is specified by the location of the matching point and the value of  $S_L/S_m$ . Thus, as one starts from the matching point ( $S_L/S_m$ ) and proceeds along the body down-stream (decreasing  $\epsilon$ ) the local Mach number increases. However  $M_L$  never quite reaches  $M_\infty$  as  $\epsilon$  approaches zero.

Figure (13) is a plot of  $q_L/q_\infty$  vs  $\epsilon$  for several values of  $M_\infty$ . Again, as one proceeds downstream the local dynamic pressure increases toward its free stream value but falls off before reaching it.

Figure (14) is a plot of  $\frac{(q/\beta)_L}{(q/\beta)_\infty}$  vs  $\epsilon$  for several values of  $M_\infty$ . Here, the combined effects of  $M_L$  and  $q_L$  cause  $(q/\beta)_L$  to be greater than  $(q/\beta)_\infty$  all along the surface except for very small  $\epsilon$  (very far aft). For  $\epsilon \approx 0$ ,  $(q/\beta)_L$  decreases to a value less than  $(q/\beta)_\infty$ . Figure (14) should be compared with figures (3) and (10) to illustrate the differences between the results of oblique shock theory, Newtonian theory, and blast wave theory.

## SECTION IV

### CONCLUSIONS

This report has attempted an approximate analysis of the degree to which various types of shock wave and expansion systems change aerodynamic flutter parameters from free stream to local conditions. The methods used are not the most sophisticated and do have definite limits on their ranges of applicability, so the reader must be wary of drawing conclusions which are too broad compared to the validity of the analyses. However, the following summarizes some of the trends obtained which appear to be reasonable.

Local Mach Number - As is already well known, the local Mach number predicted by oblique shock theory can be considerably less than the original free stream value. The opposite effect for a supersonic expansion is also well known and will not be belabored here. In regions where the modified form of Newtonian theory would apply (i.e., blunt noses or large angles of attack) the local Mach number (again, as well known) turns out to be much less than one would predict with oblique shock theory. In regions where the blast wave theory would apply (i.e., surface regions behind a blunted nose), the local Mach number starts to recover from its large losses sustained in the region of the blunt nose but never quite reaches its free stream value as the flow moves over the aft regions of the body.

Local Dynamic Pressure - Generally speaking, as angle of attack increases, the effect of an attendant oblique shock wave is to increase the local dynamic pressure to a value approaching as much as six times its free stream value for  $\gamma = 1.4$ . However, as angle of attack is increased beyond a certain point the local dynamic pressure then starts to decrease back toward its free stream value. In expansion regions, the local dynamic pressure is almost always less than the free stream dynamic pressure. In regions where the modified form of Newtonian theory applies, the trend is the same as for an oblique shock. However, due to the large losses in momentum in passing through the nose shock, the local dynamic pressure starts out at a low level and never quite reaches its free stream value. Farther aft, where the blast wave theory applies, one can again see how the local dynamic pressure never attains its free stream value, regardless of where the blast wave solution is matched to the nose conditions.

The Flutter Parameter,  $q/\beta$  - The analysis for the oblique shock wave revealed that  $q/\beta$  always is greater locally than in the free stream. Thus one would conclude that certain flutter problems may be quite serious even though the free stream conditions would indicate freedom from flutter. In expansion regions  $q/\beta$  is always less locally than in the free stream, therefore indicating a stabilizing effect on flutter. In the regions where the modified form of Newtonian flow theory could be applied,  $q/\beta$  locally is always greater than its free stream value.

Figure (10) does show a small region where the opposite is true, but that effect is at such small values of  $\delta$  that the theory would not be valid. In regions where blast theory applies,  $q/\beta$  is generally much larger locally than in the free stream, however,  $q/\beta$  does fall to values less than in the free stream as the flow moves very far aft.

Finally, while we recognize the limitations in this analysis, it is still apparent that local aerodynamic conditions can be significantly different from those in the free stream. This study indicates then that these changes in important aerodynamic conditions should be carefully considered in the design analysis of supersonic and hypersonic aircraft and missiles. The results of this program should give some preliminary information to the designer until more sophisticated analyses are employed or until experimental data becomes available.

## REFERENCES

1. Ames Research Staff, "Equations, Tables, and Charts for Compressible Flow", NACA Report 1135; 1953
2. Buck, M. L. and McLaughlin, E. S., "Aerodynamic Prediction Techniques for Hypersonic Winged Re-entry Vehicles", ASRMDF-TM-62-5; 1963
3. Lee, J. D., "Pressures on the Blunt Flat Plates in Hypersonic and Supersonic Flows", FDL-TDR-64-102; 1964
4. Vann, W. D., "Hypersonic Flow over Blunt Slab Wings with Sweep Angles from 0 to 70°", ARL-TR-64-171; 1964

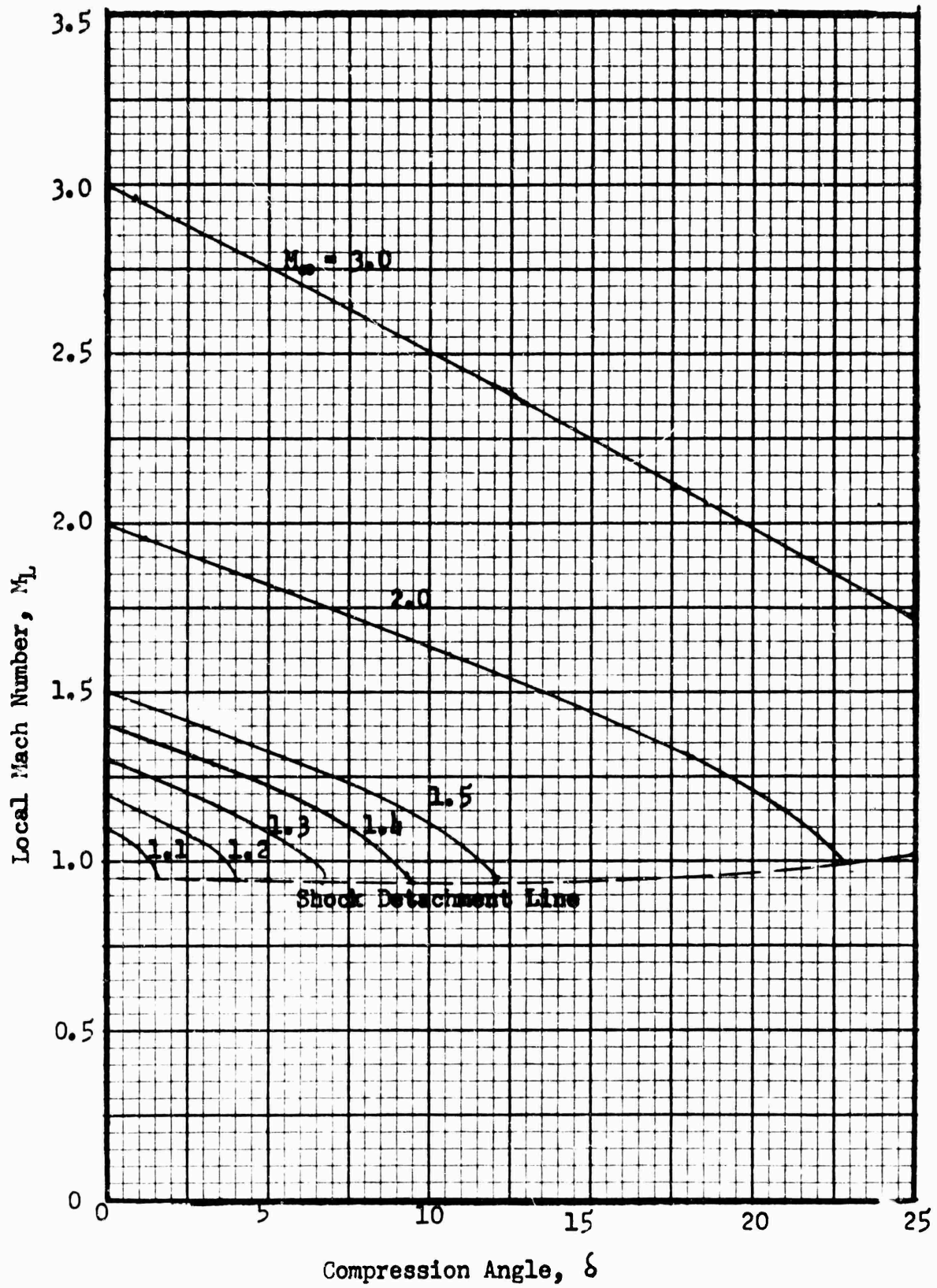


Figure 1(a). Local Mach Number vs Compression Angle, Oblique Shock Theory

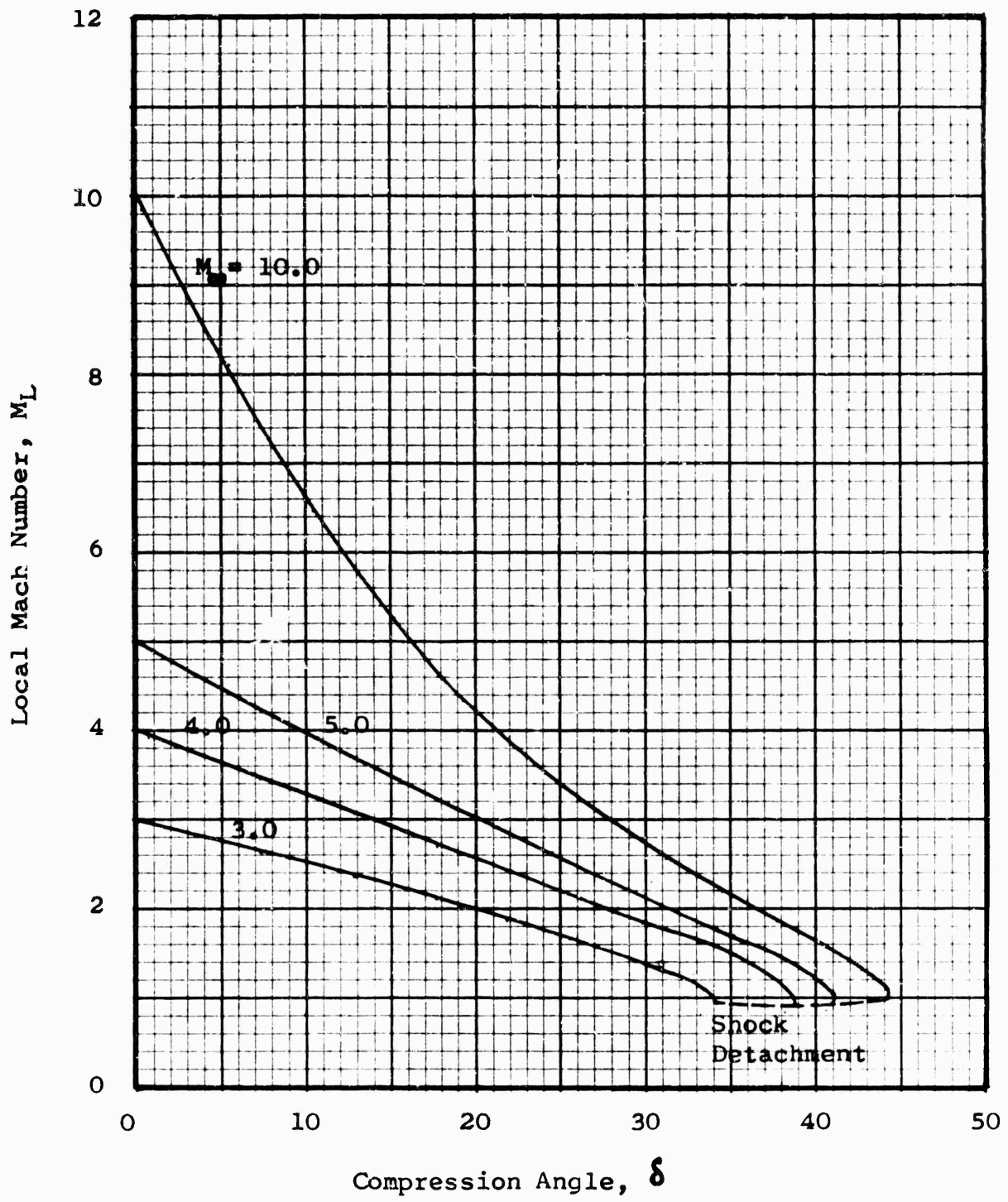


Figure 1(b). Local Mach Number vs Compression Angle, Oblique Shock Theory

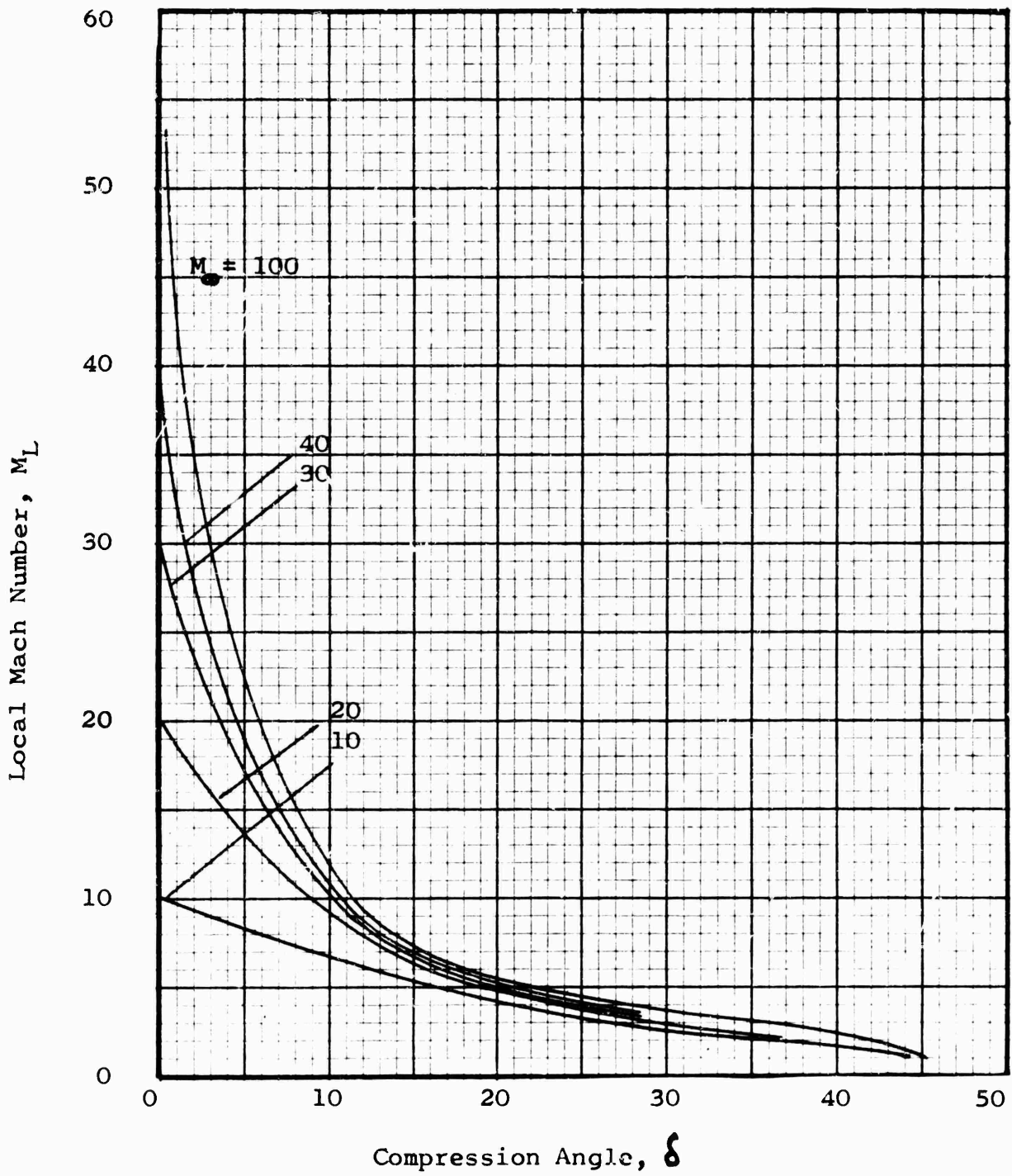


Figure 1(c). Local Mach Number vs Compression Angle, Oblique Shock Theory

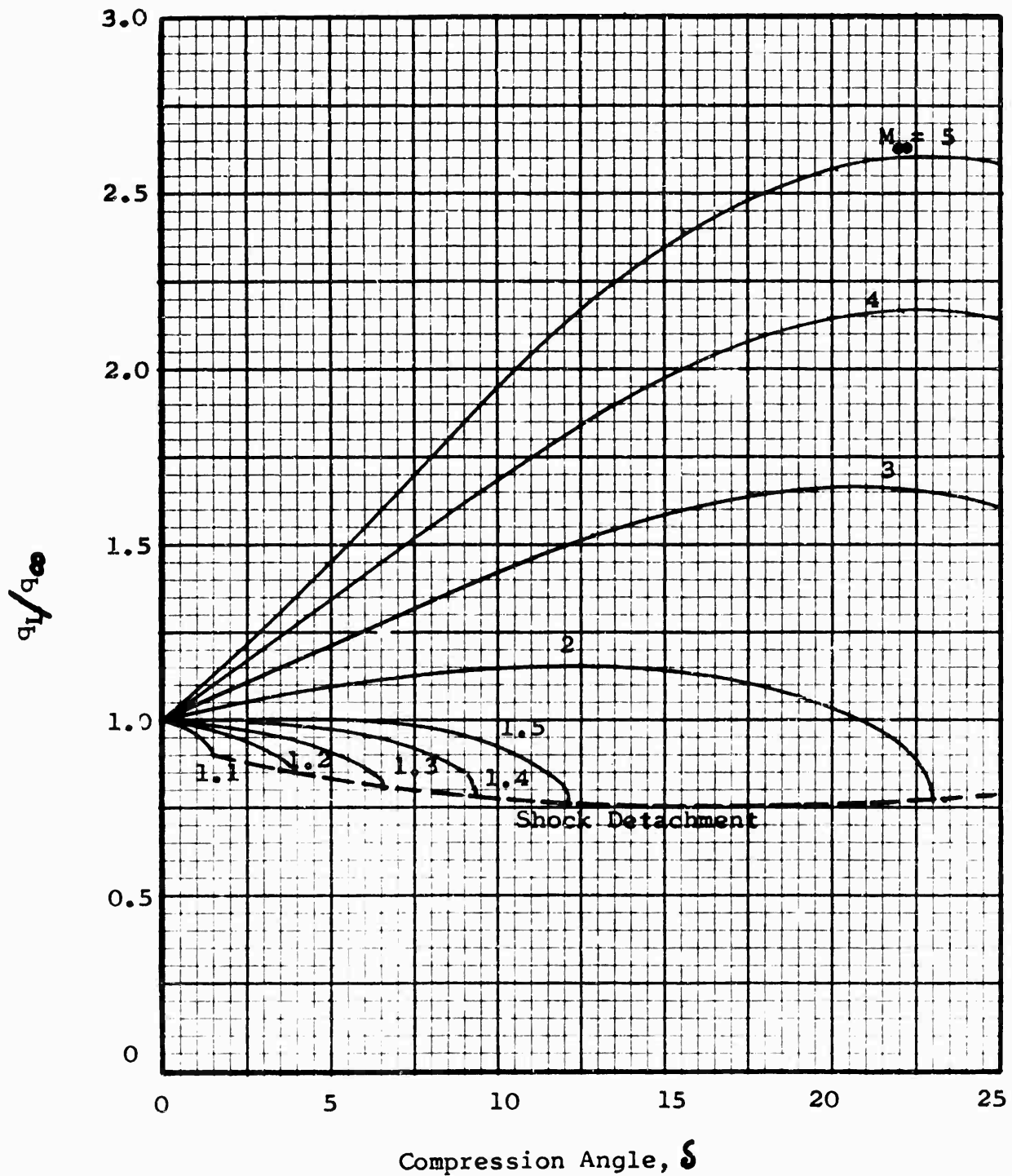


Figure 2(a). Ratio of Local Dynamic Pressure to Free Stream Dynamic Pressure vs Compression Angle, Oblique Shock Theory

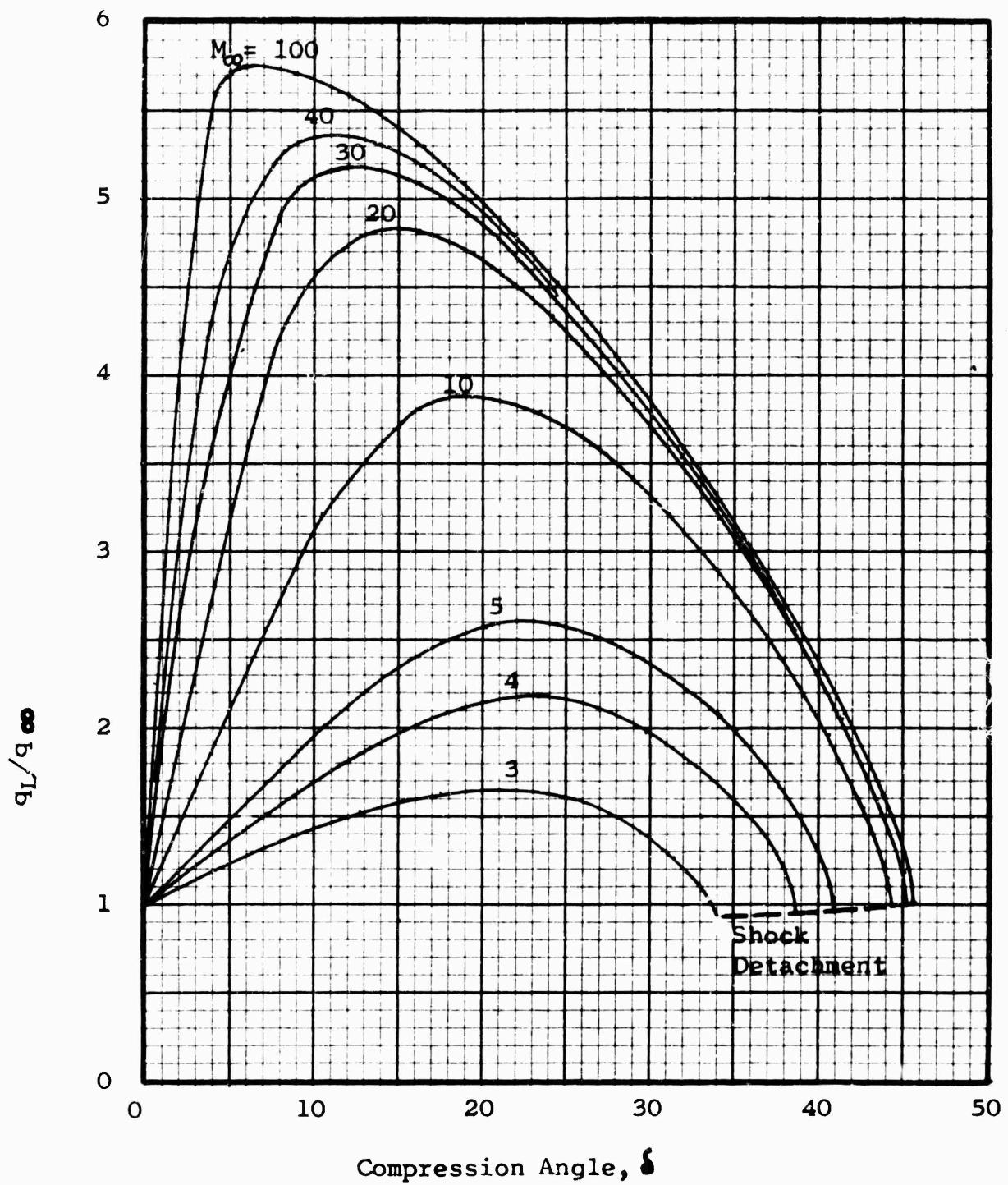


Figure 2(b). Ratio of Local Dynamic Pressure to Free Stream Dynamic Pressure vs Compression Angle, Oblique Shock Theory

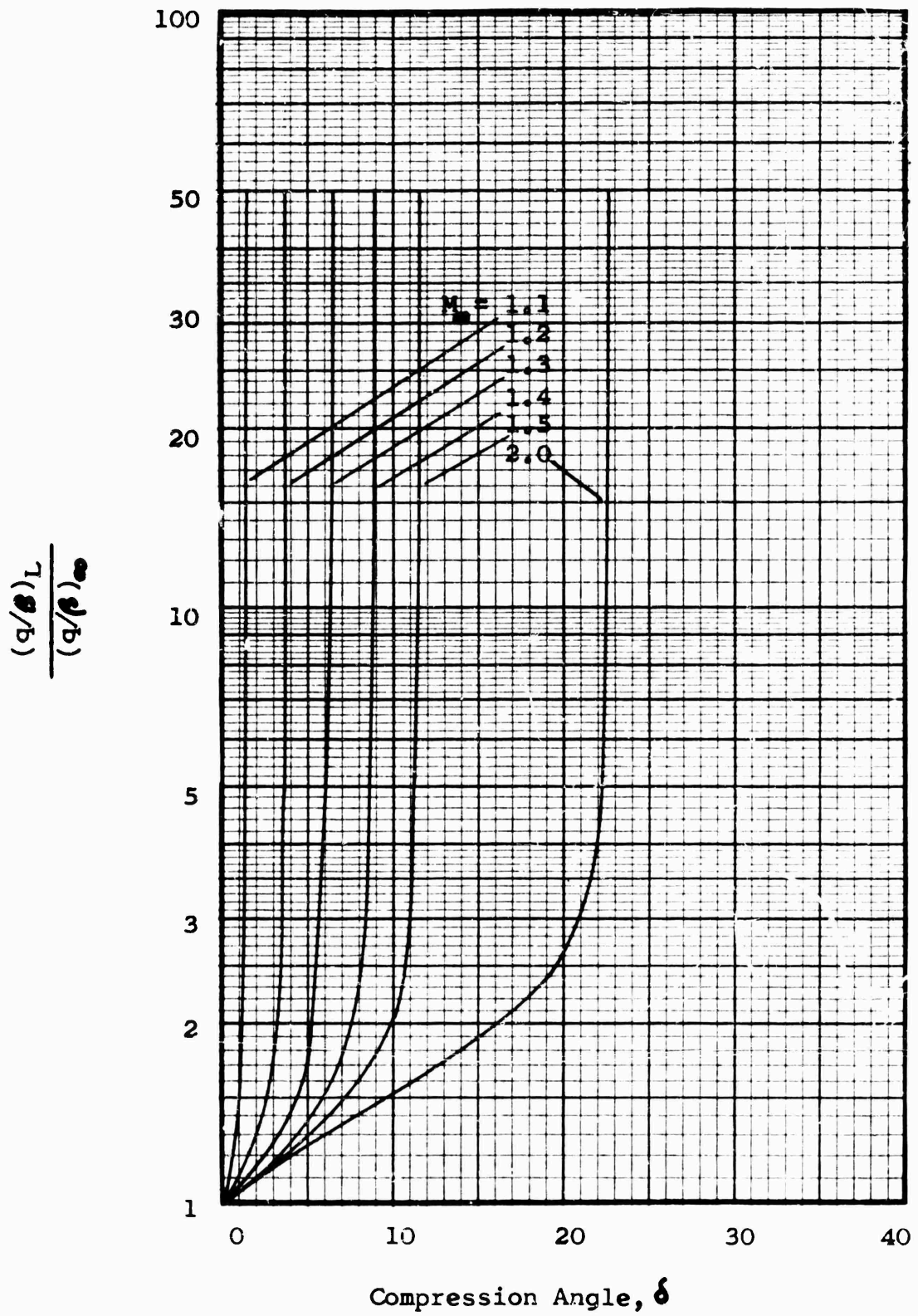


Figure 3(a). Ratio of  $(q/\rho)_L$  to  $(q/\rho)_\infty$  vs Compression Angle, Oblique Shock Theory

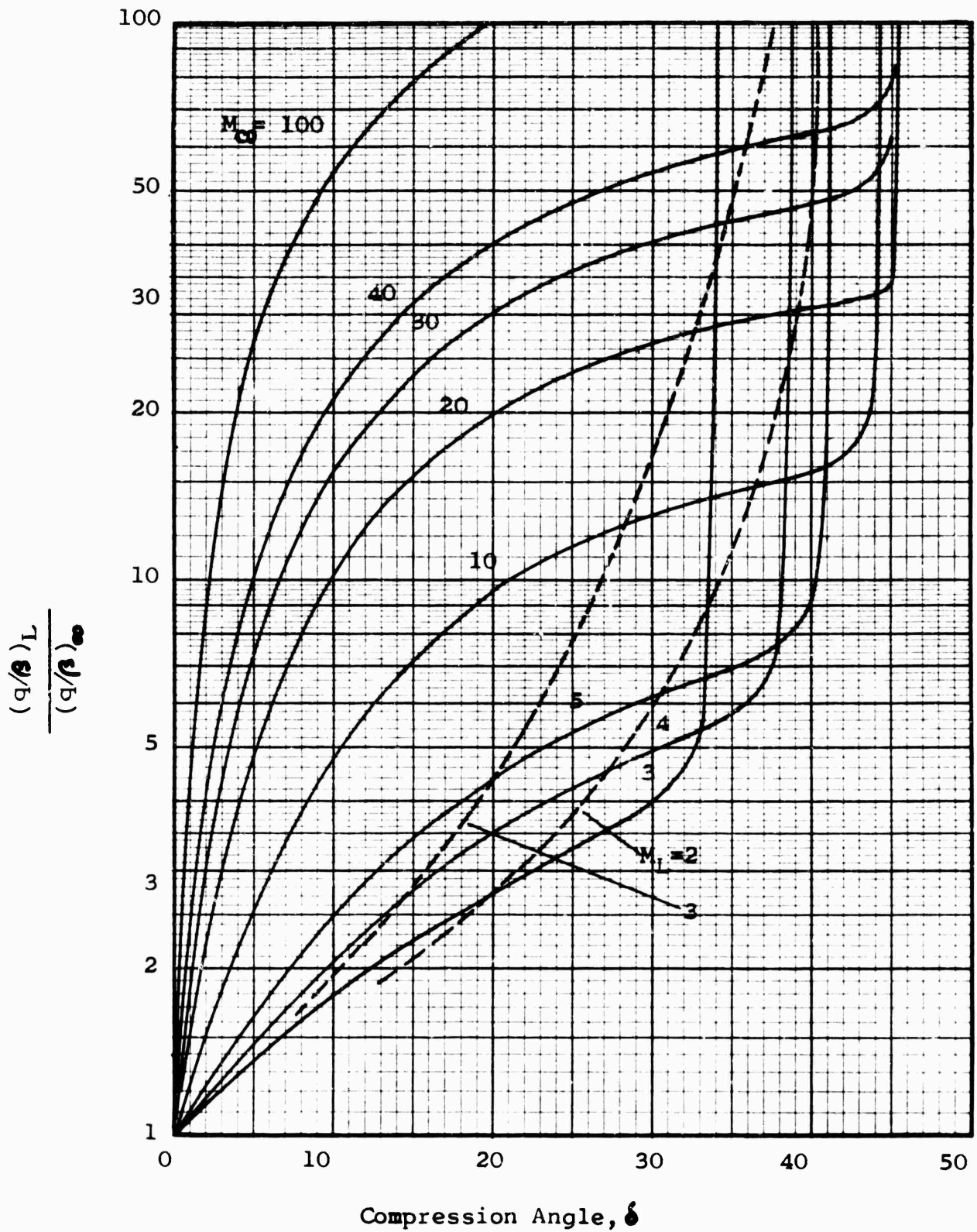


Figure 3(b). Ratio of  $(q/\rho)_L$  to  $(q/\rho)_\infty$  vs Compression Angle, Oblique Shock Theory

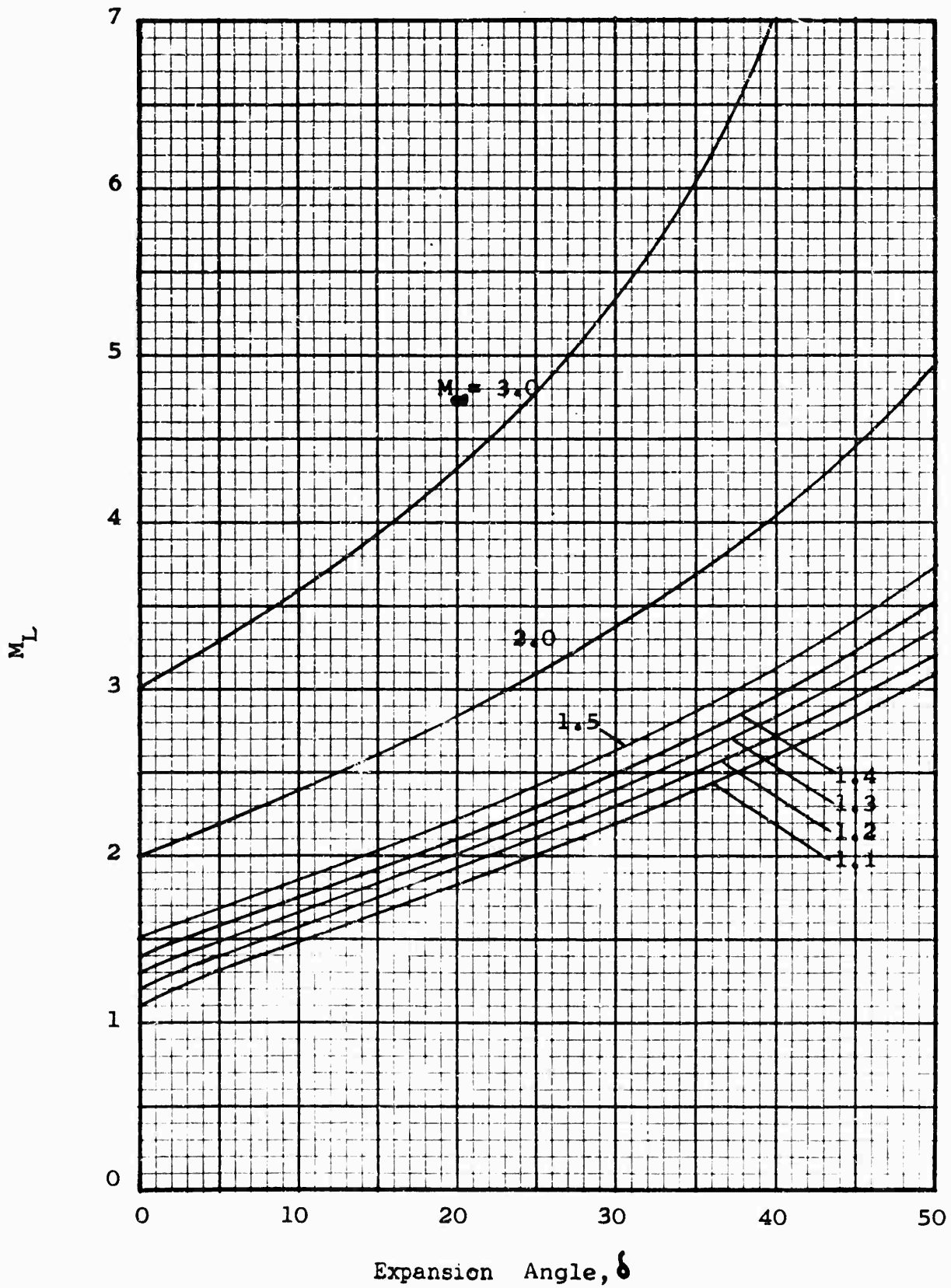


Figure 4(a). Local Mach Number vs Expansion Angle, Prandtl-Meyer Expansion

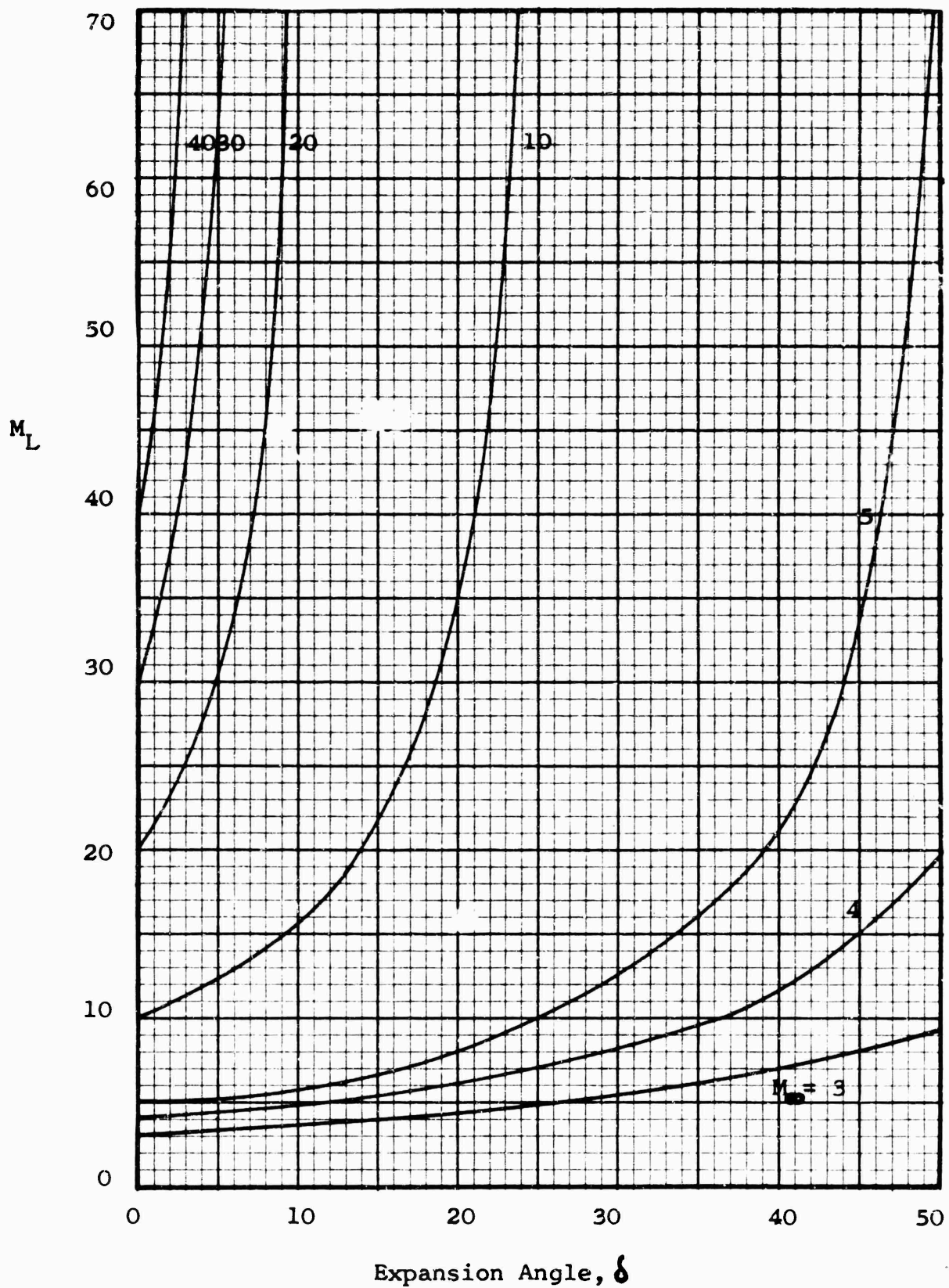


Figure 4(b). Local Mach Number vs Expansion Angle, Prandtl-Meyer Expansion

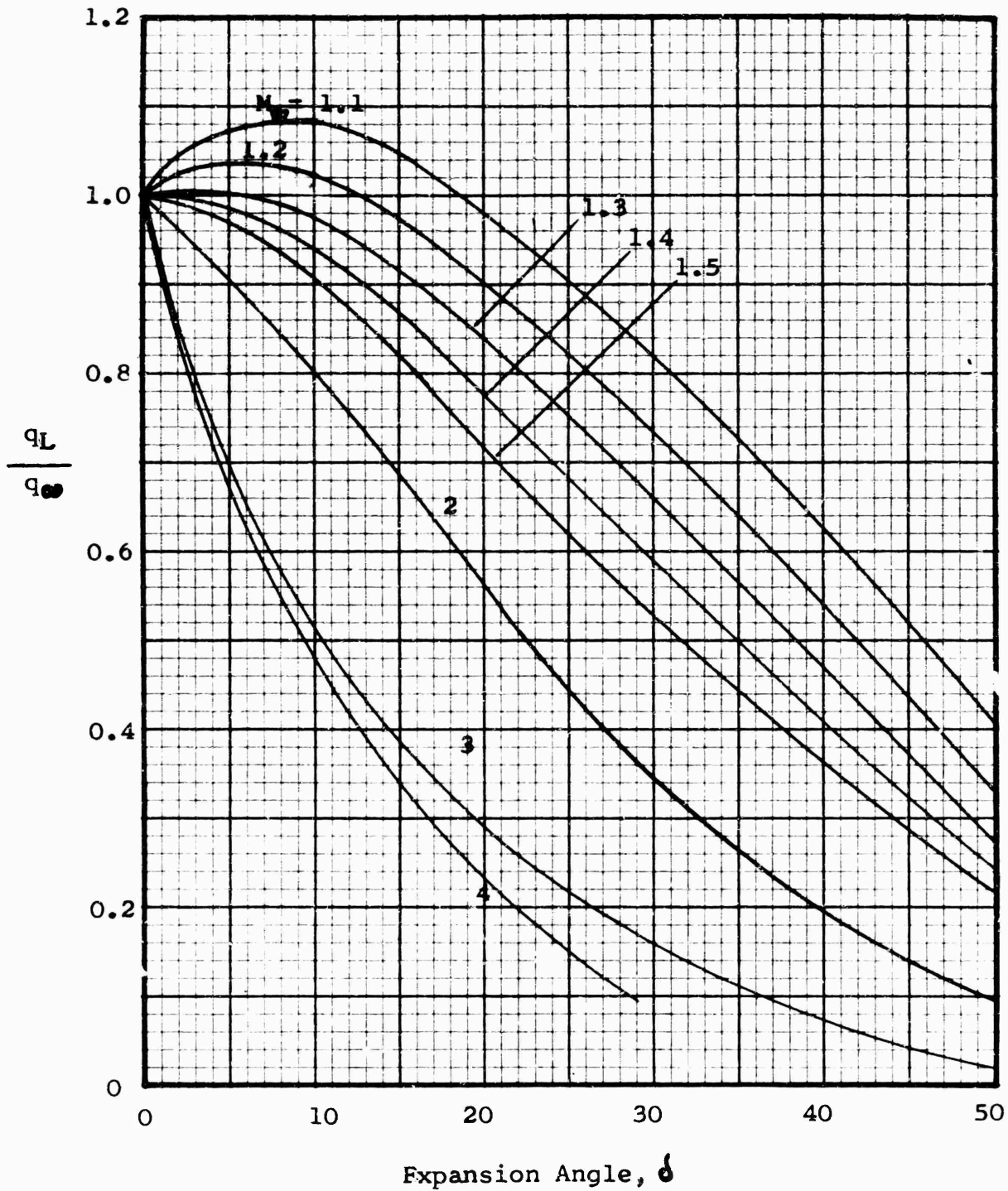


Figure 5(a). Ratio of Local Dynamic Pressure to Free Stream Dynamic Pressure vs Expansion Angle, Prandtl-Meyer Expansion

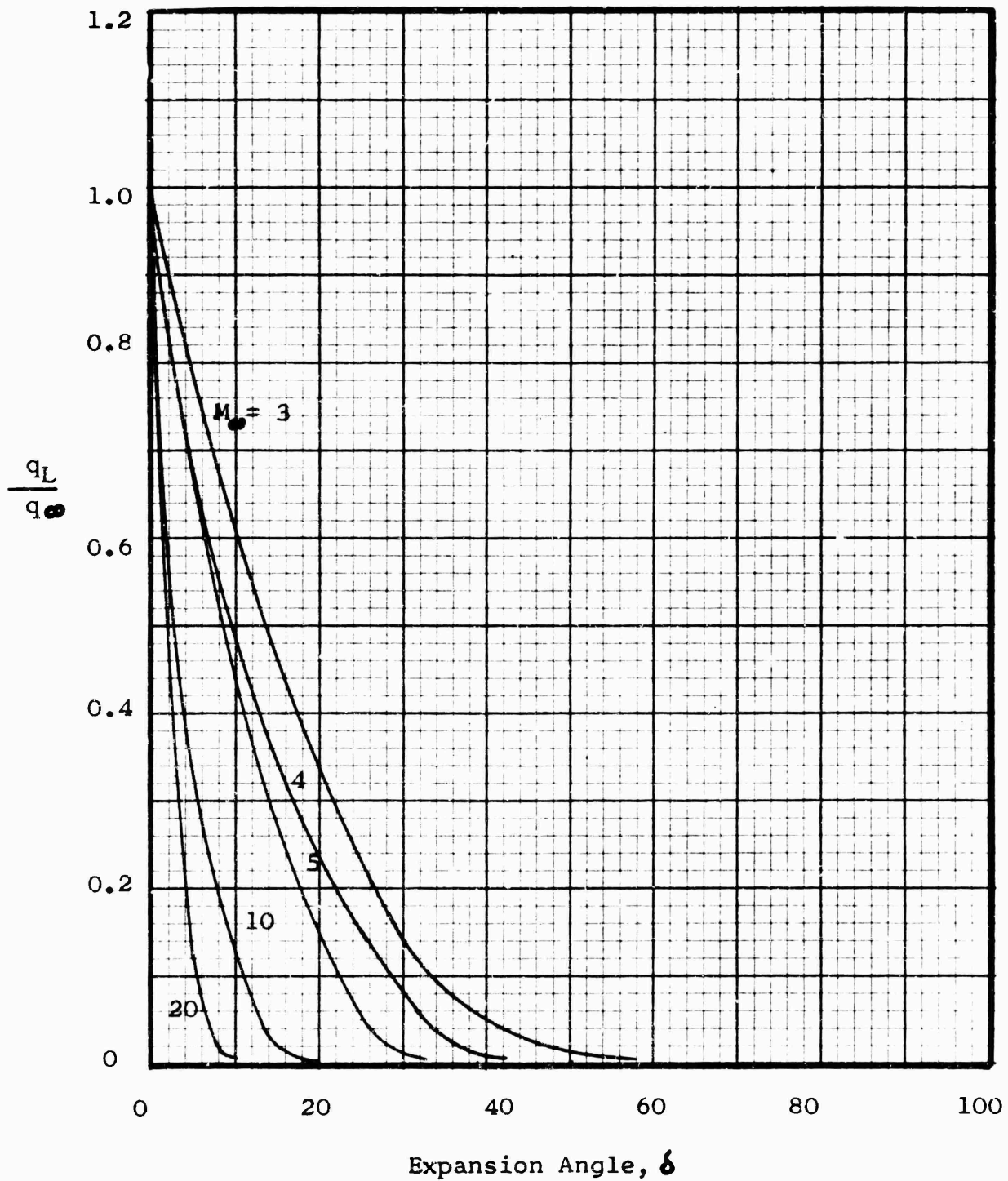


Figure 5(b). Ratio of Local Dynamic Pressure to Free Stream Dynamic Pressure vs Expansion Angle, Prandtl-Meyer Expansion

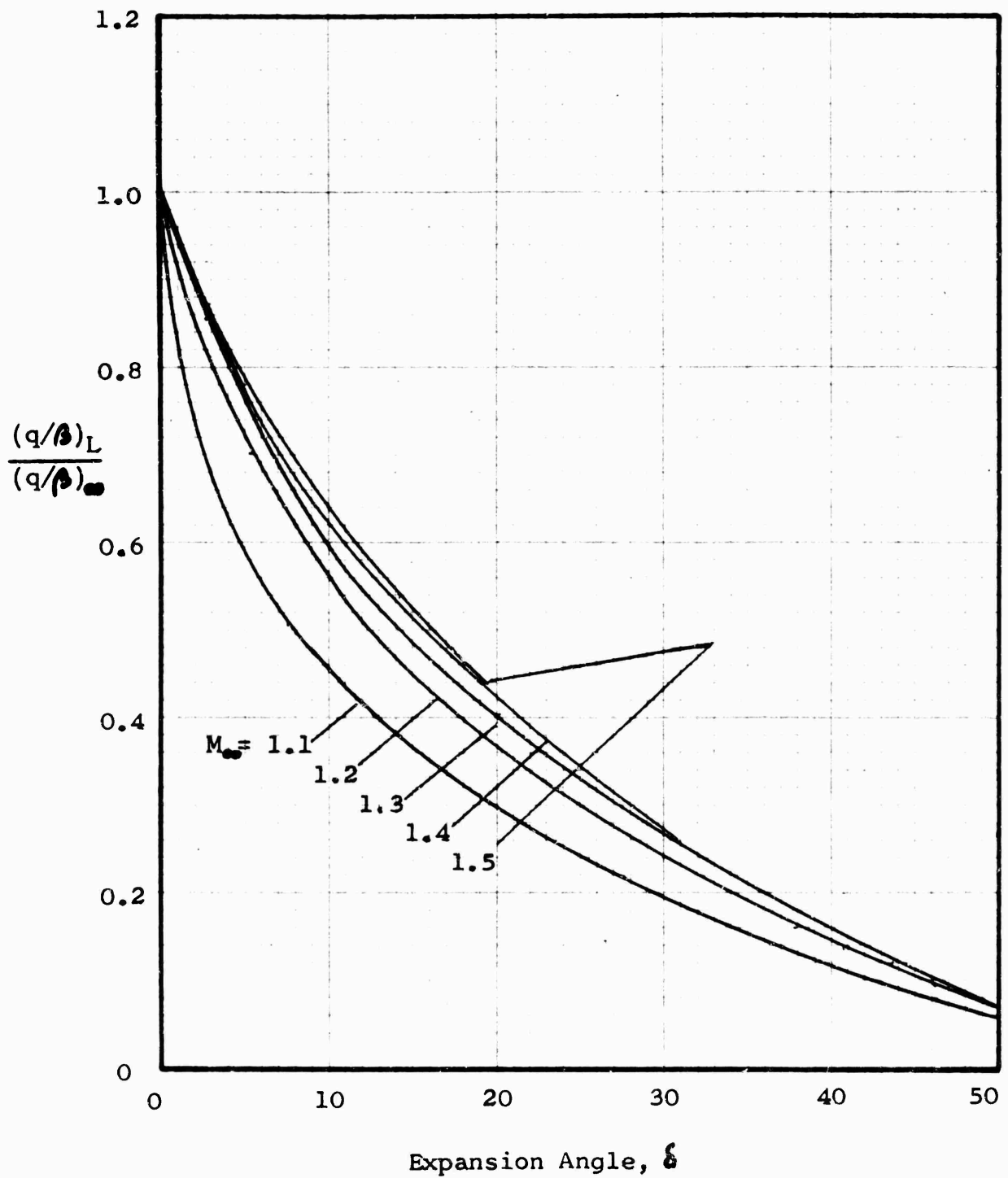


Figure 6(a). Ratio of  $(q/\rho)_L$  to  $(q/\rho)_\infty$  vs Expansion Angle, Prandtl-Meyer Expansion

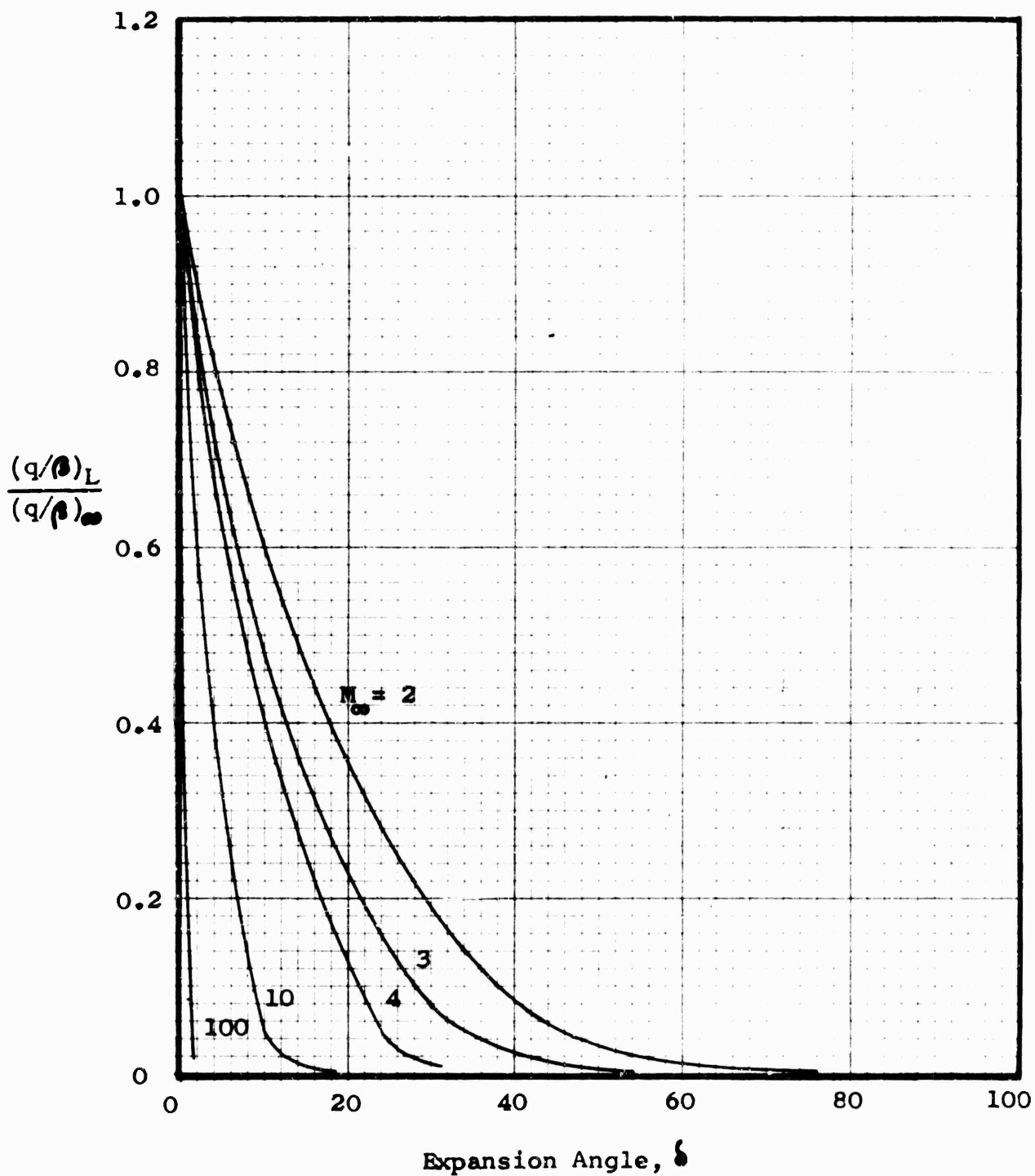


Figure 6(b). Ratio of  $(q/\rho)_L$  to  $(q/\rho)_\infty$  vs Expansion Angle, Prandtl-Meyer Expansion

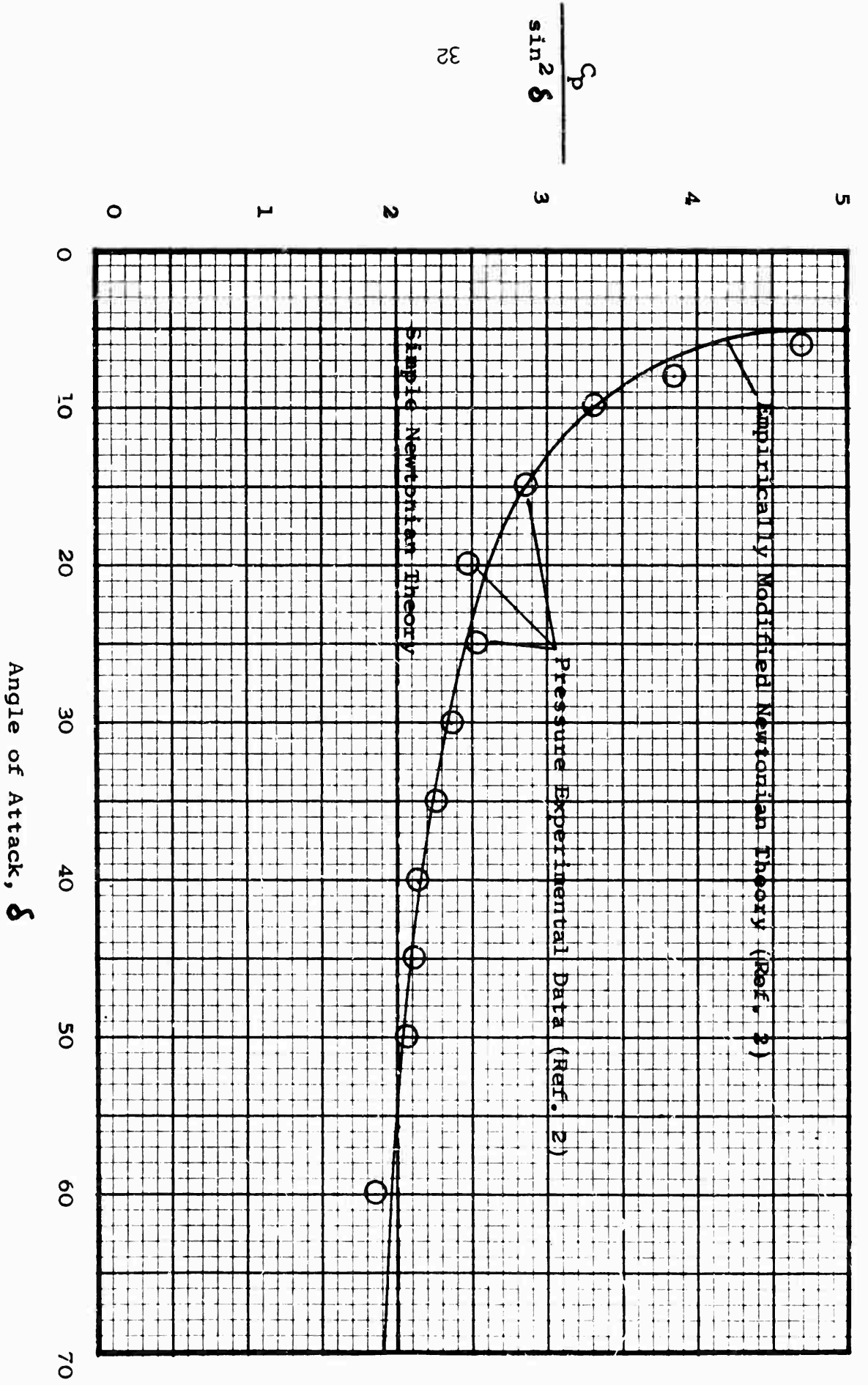


Figure 7. Correlation of Simple and Modified Forms of Newtonian Theory with Experimental Results

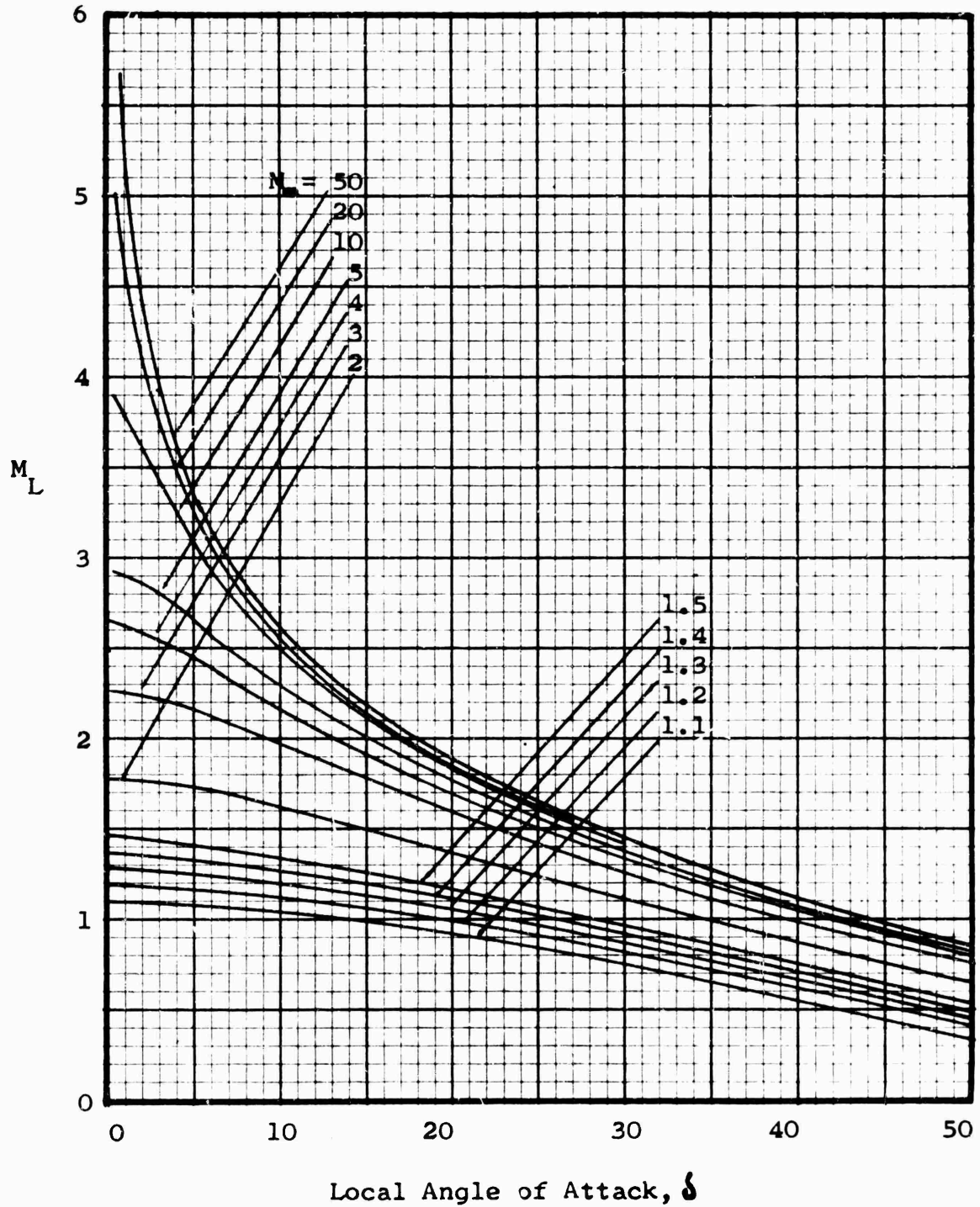


Figure 8. Local Mach Number vs Local Angle of Attack, Modified Newtonian Theory

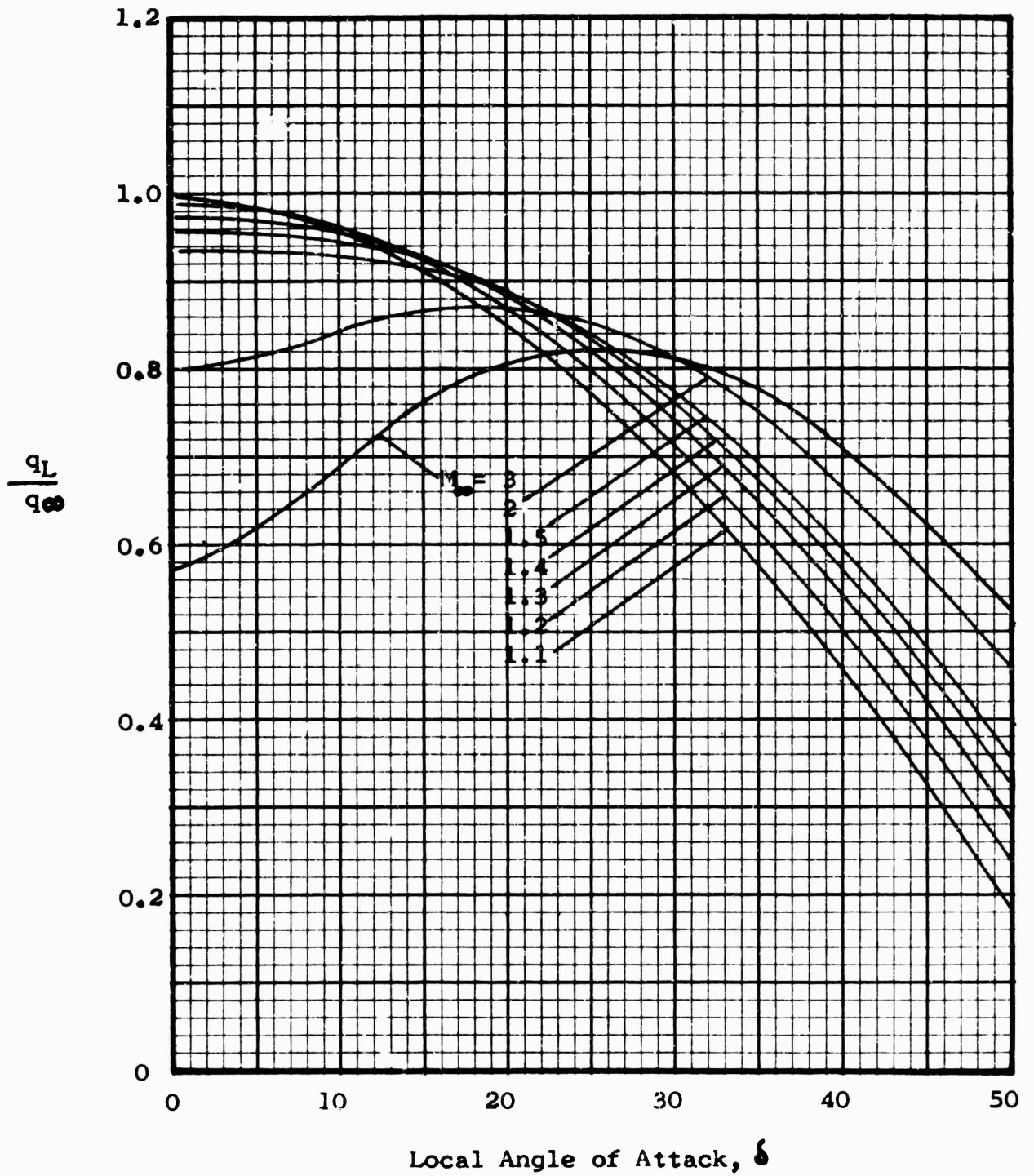


Figure 9(a). Ratio of Local Dynamic Pressure to Free Stream Dynamic Pressure vs Local Angle of Attack, Modified Newtonian Theory

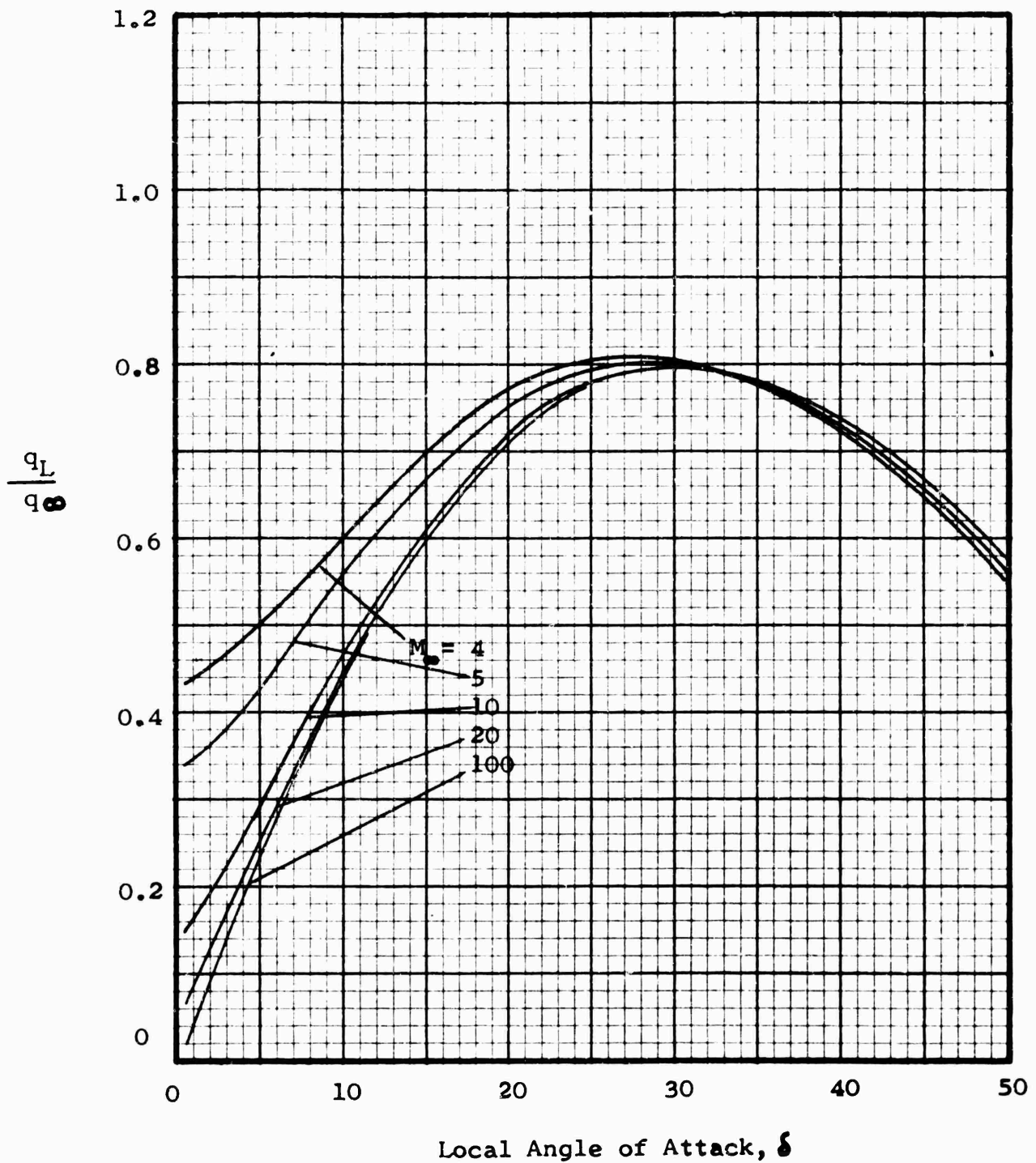


Figure 9(b). Ratio of Local Dynamic Pressure to Free Stream Dynamic Pressure vs Local Angle of Attack, Modified Newtonian Theory

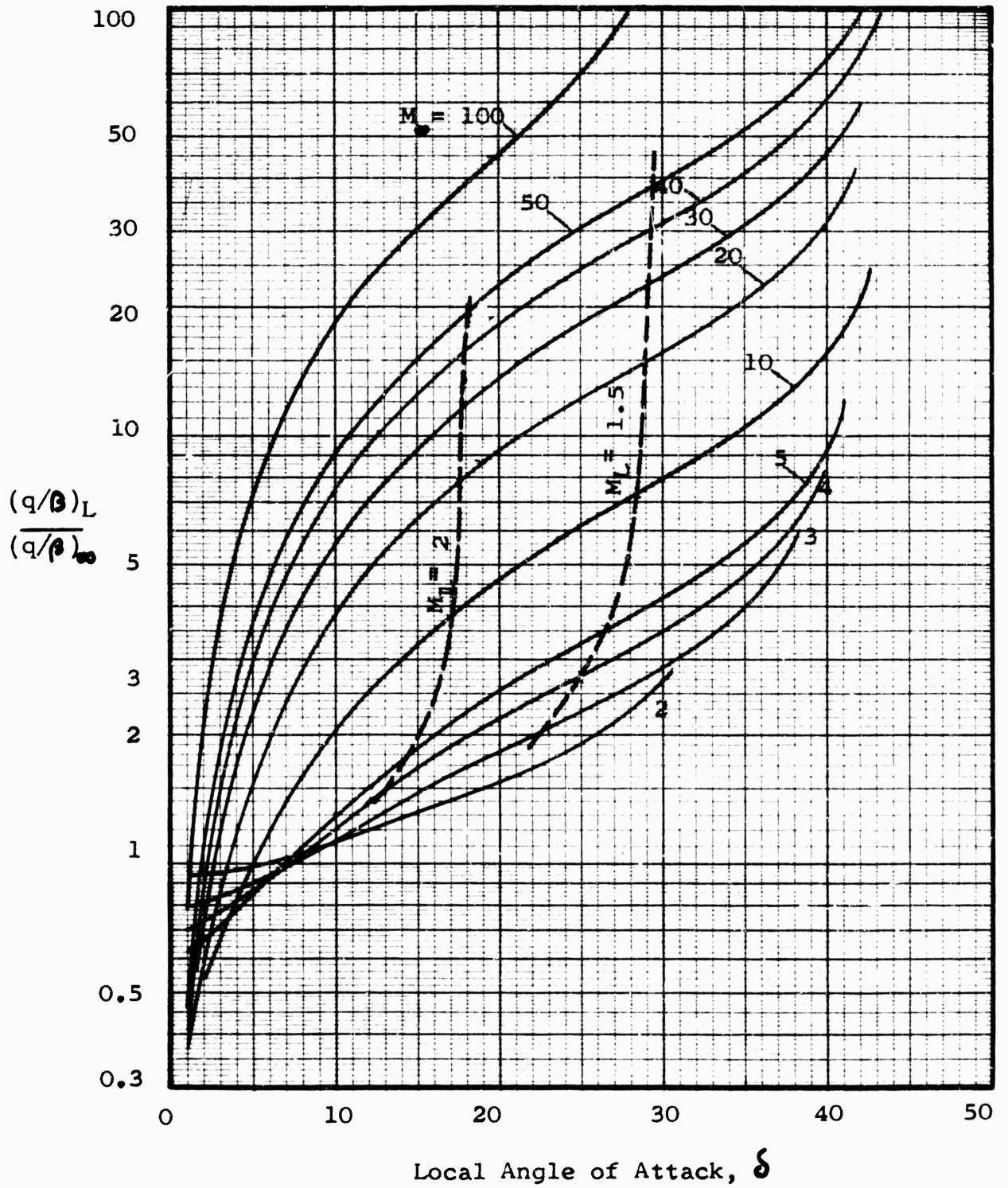


Figure 10. Ratio of  $(q/\beta)_L$  to  $(q/\beta)_\infty$  vs Local Angle of Attack, Modified Newtonian Theory

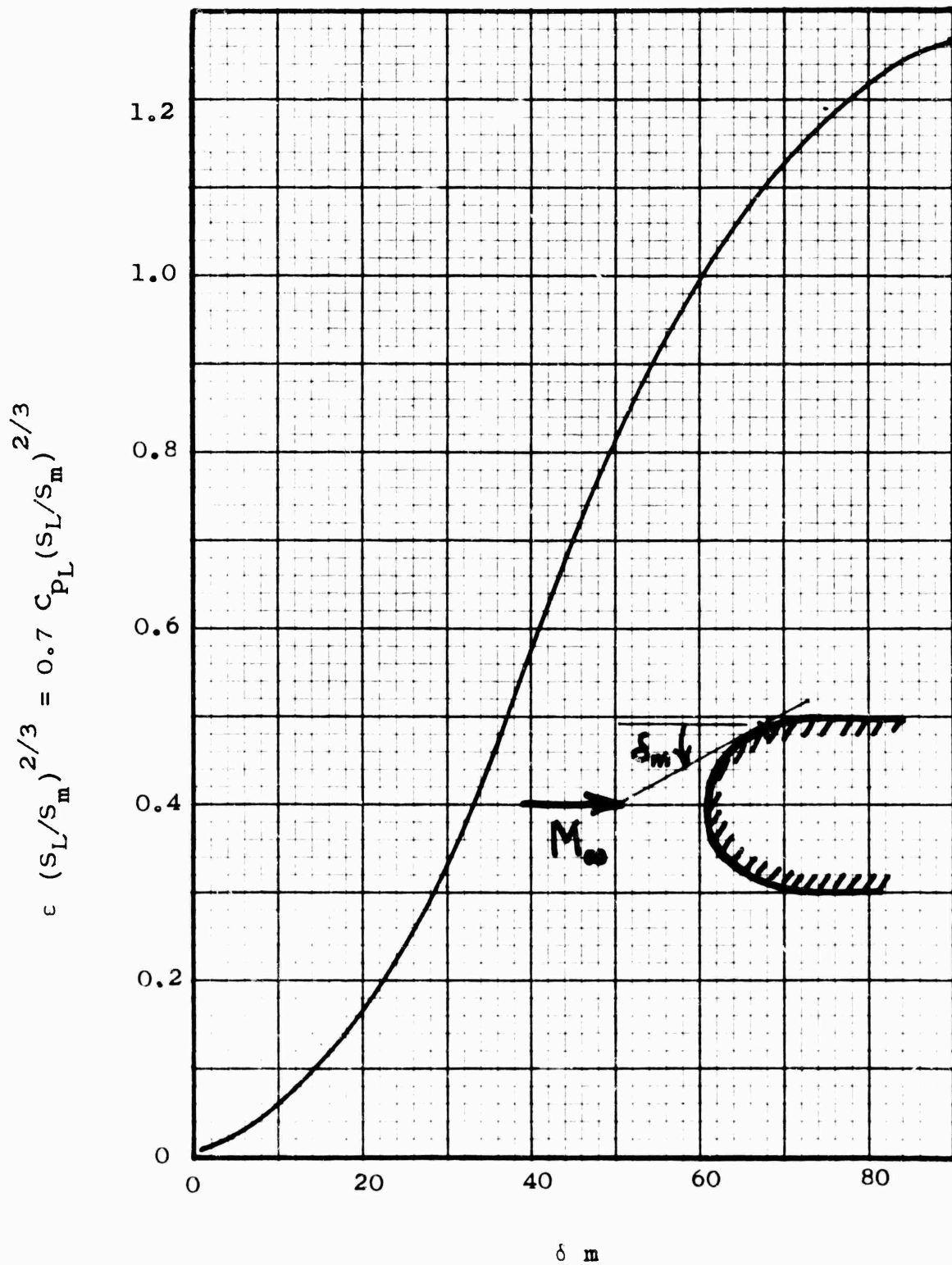


Figure 11. The Dependence of Local Pressure on the Location of the Newtonian-Blast Theory Matching Point

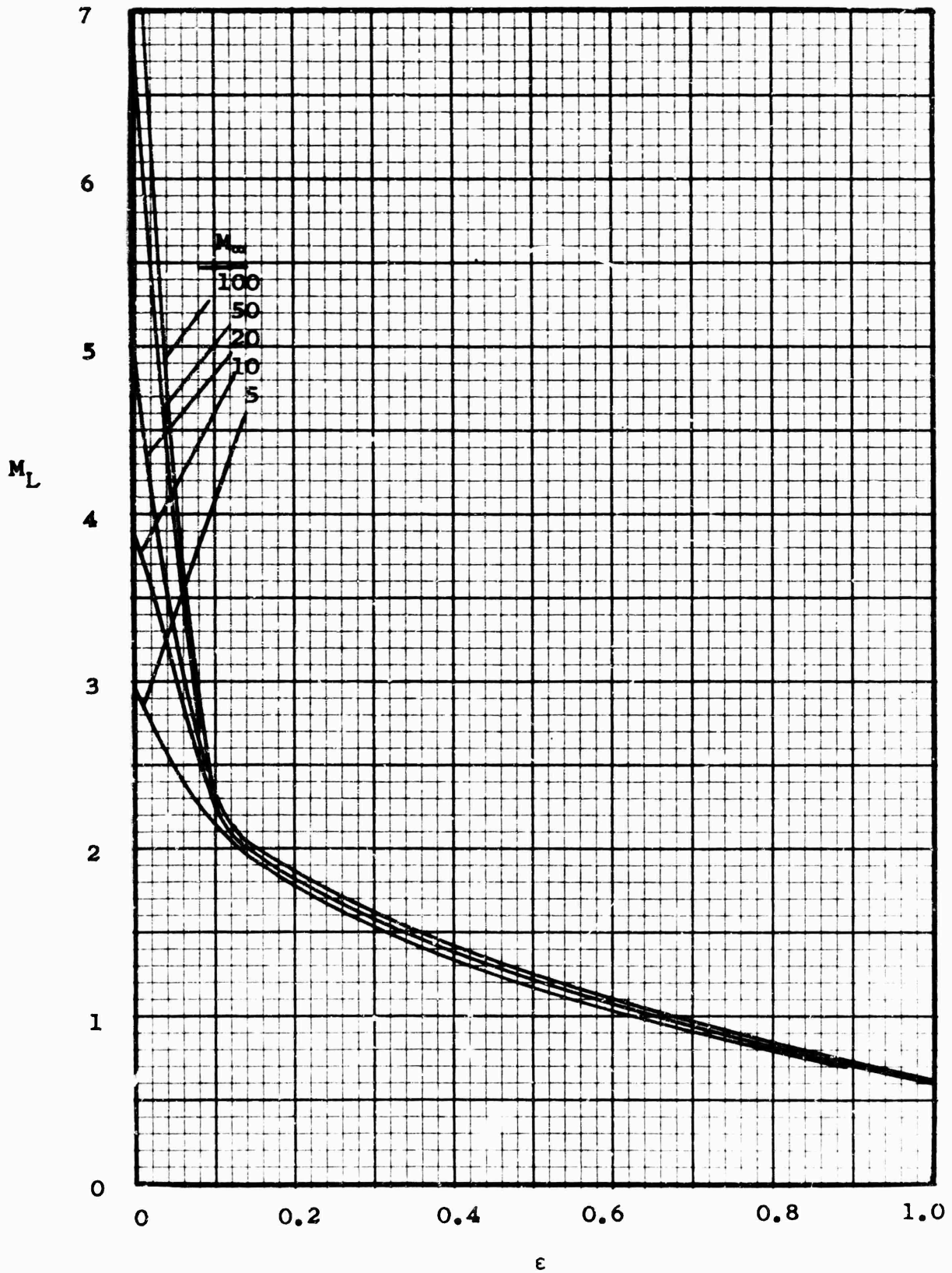


Figure 12. Local Mach Number vs the Matching Parameter, Blast Wave Theory Matched with Newtonian Theory

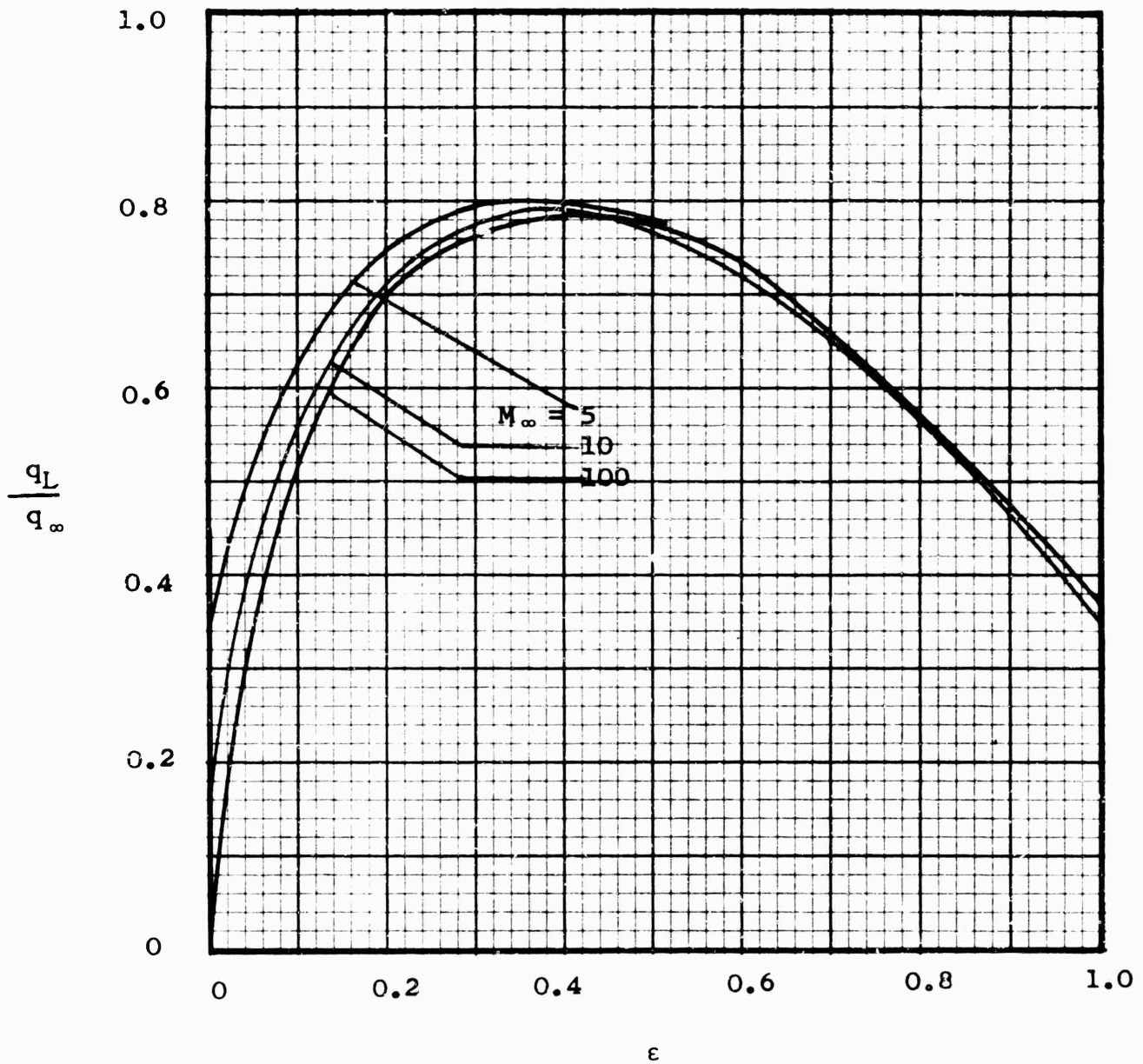


Figure 13. The Ratio of Local Dynamic Pressure to Free Stream Dynamic Pressure vs the Matching Parameter  $\epsilon$ , Blast Wave Theory Matched with Newtonian Theory

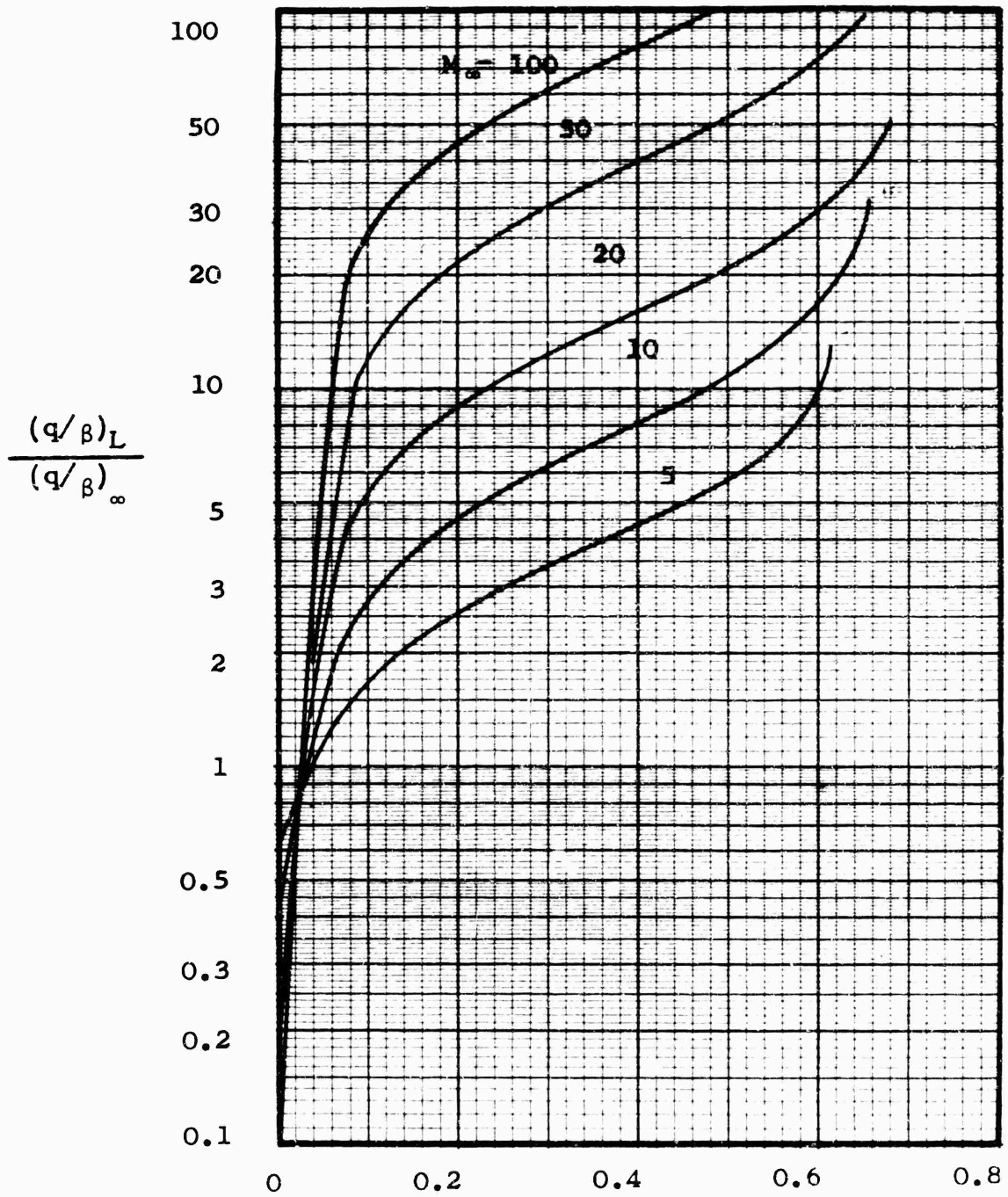


Figure 14. The ratio  $(q/\beta)_L$  to  $(q/\beta)_\infty$  vs the Matching parameter  $\epsilon$ , Blast Wave Theory Matched with Newtonian Theory

~~UNCLASSIFIED~~  
Security Classification

DOCUMENT CONTROL DATA - R&D		
<i>(Security classification of title, body of abstract and indexing annotation must be entered when the overall report is classified)</i>		
1. ORIGINATING ACTIVITY (Corporate author) Aerospace Dynamics Branch Vehicle Dynamics Division Air Force Flight Dynamics Laboratory		2a. REPORT SECURITY CLASSIFICATION UNCLASSIFIED
		2b. GROUP
3. REPORT TITLE Local Aerodynamic Parameters for Supersonic and Hypersonic Flutter Analyses		
4. DESCRIPTIVE NOTES (Type of report and inclusive dates) 1 July 1964 to 1 April 1965 Report to advance the state-of-the-art of flutter prediction for flight vehicles.		
5. AUTHOR(S) (Last name, first name, initial) Olsen, James J.		
5. REPORT DATE October 1965	7a. TOTAL NO. OF PAGES 40	7b. NO. OF REFS 4
8a. CONTRACT OR GRANT NO.	8a. ORIGINATOR'S REPORT NUMBER(S) AFFDL-TR-65-183	
b. PROJECT NO. 1370		
c. Task No. 137003	8b. OTHER REPORT NO(S) (Any other numbers that may be assigned this report)	
d.		
10. AVAILABILITY/LIMITATION NOTICES Distribution of this document is Unlimited		
11. SUPPLEMENTARY NOTES	12. SPONSORING MILITARY ACTIVITY Air Force Flight Dynamics Laboratory	
13. ABSTRACT This report presents the results of an analysis to determine how certain aerodynamic flutter parameters ( $M$ , $q$ , $q/\beta$ ) are changed from their free stream values by the existence of supersonic and hypersonic nose shock waves and expansions. The results indicate that nose shock waves and expansions can create a new set of "free stream" conditions for flutter analyses. These new free stream conditions can be sufficiently different from the undisturbed "free stream" condition to warrant their detailed analyses in the supersonic and hypersonic vehicle.		

**Security Classification**

14. KEY WORDS	LINK A		LINK B		LINK C	
	ROLE	WT	ROLE	WT	ROLE	WT

**INSTRUCTIONS**

**1. ORIGINATING ACTIVITY:** Enter the name and address of the contractor, subcontractor, grantee, Department of Defense activity or other organization (*corporate author*) issuing the report.

**2a. REPORT SECURITY CLASSIFICATION:** Enter the overall security classification of the report. Indicate whether "Restricted Data" is included. Marking is to be in accordance with appropriate security regulations.

**2b. GROUP:** Automatic downgrading is specified in DoD Directive 5200.10 and Armed Forces Industrial Manual. Enter the group number. Also, when applicable, show that optional markings have been used for Group 3 and Group 4 as authorized.

**3. REPORT TITLE:** Enter the complete report title in all capital letters. Titles in all cases should be unclassified. If a meaningful title cannot be selected without classification, show title classification in all capitals in parenthesis immediately following the title.

**4. DESCRIPTIVE NOTES:** If appropriate, enter the type of report, e.g., interim, progress, summary, annual, or final. Give the inclusive dates when a specific reporting period is covered.

**5. AUTHOR(S):** Enter the name(s) of author(s) as shown on or in the report. Enter last name, first name, middle initial. If military, show rank and branch of service. The name of the principal author is an absolute minimum requirement.

**6. REPORT DATE:** Enter the date of the report as day, month, year, or month, year. If more than one date appears on the report, use date of publication.

**7a. TOTAL NUMBER OF PAGES:** The total page count should follow normal pagination procedures, i.e., enter the number of pages containing information.

**7b. NUMBER OF REFERENCES:** Enter the total number of references cited in the report.

**8a. CONTRACT OR GRANT NUMBER:** If appropriate, enter the applicable number of the contract or grant under which the report was written.

**8b, 8c, & 8d. PROJECT NUMBER:** Enter the appropriate military department identification, such as project number, subproject number, system numbers, task number, etc.

**9a. ORIGINATOR'S REPORT NUMBER(S):** Enter the official report number by which the document will be identified and controlled by the originating activity. This number must be unique to this report.

**9b. OTHER REPORT NUMBER(S):** If the report has been assigned any other report numbers (*either by the originator or by the sponsor*), also enter this number(s).

**10. AVAILABILITY/LIMITATION NOTICES:** Enter any limitations on further dissemination of the report, other than those

imposed by security classification, using standard statements such as:

- (1) "Qualified requesters may obtain copies of this report from DDC."
- (2) "Foreign announcement and dissemination of this report by DDC is not authorized."
- (3) "U. S. Government agencies may obtain copies of this report directly from DDC. Other qualified DDC users shall request through \_\_\_\_\_."
- (4) "U. S. military agencies may obtain copies of this report directly from DDC. Other qualified users shall request through \_\_\_\_\_."
- (5) "All distribution of this report is controlled. Qualified DDC users shall request through \_\_\_\_\_."

If the report has been furnished to the Office of Technical Services, Department of Commerce, for sale to the public, indicate this fact and enter the price, if known.

**11. SUPPLEMENTARY NOTES:** Use for additional explanatory notes.

**12. SPONSORING MILITARY ACTIVITY:** Enter the name of the departmental project office or laboratory sponsoring (*paying for*) the research and development. Include address.

**13. ABSTRACT:** Enter an abstract giving a brief and factual summary of the document indicative of the report, even though it may also appear elsewhere in the body of the technical report. If additional space is required, a continuation sheet shall be attached.

It is highly desirable that the abstract of classified reports be unclassified. Each paragraph of the abstract shall end with an indication of the military security classification of the information in the paragraph, represented as (TS), (S), (C), or (U).

There is no limitation on the length of the abstract. However, the suggested length is from 150 to 225 words.

**14. KEY WORDS:** Key words are technically meaningful terms or short phrases that characterize a report and may be used as index entries for cataloging the report. Key words must be selected so that no security classification is required. Identifiers, such as equipment model designation, trade name, military project code name, geographic location, may be used as key words but will be followed by an indication of technical context. The assignment of links, rules, and weights is optional.